BR111567
ARE TR89311
JULY 1989
COPY No 26

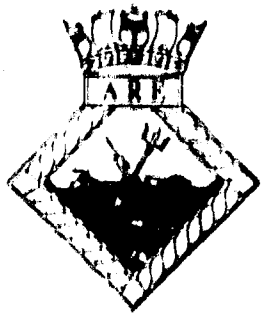

WAVES IN SHIP TANKS

PART 1: GENERATING A RANDOM SEA

D K Fryer

ADMIRALTY RESEARCH ESTABLISHMENT
Procurement Executive Ministry of Defence
Haslar GOSPORT Hants PO12 2AG

CONDITIONS OF RELEASE

0051802 BR-111537

********** U

********** Y

Reports quoted are not necessarily available to members of the public or to commercial organisations.

ARE TR89311

July 1989

WAVES IN SHIP TANKS

PART 1: GENERATING A RANDOM SEA

BY

D K Fryer

Summary

This report describes the difficulties encountered when modelling regular and random seas in a ship tank. A method of experiment design which minimises the errors in the sea state is proposed. One implementation of the method is described in some detail.

Admiralty Research Establishment
Haslar Gosport Hants PO12 2AG

WAVES IN SHIP TANKS

1. INTRODUCTION

The use of scale models for predicting the performance of both ships and stationary marine structures has been developed over a period of more than 100 years. The technique is based on the matching of one, or more, of the dimension less parameters listed below between the model and the full scale ship or structure.

Reynolds number, $R_n = \rho \frac{VL}{\mu}$

Froude number, $F_n = \left[\frac{V^2}{gL}\right]^{\frac{1}{2}}$

Weber number, $W_n = \rho \frac{VL^2}{\sigma}$

Mach number, $M = \left[\frac{\rho V^2}{E}\right]^{\frac{1}{2}} = \frac{V}{c}$ $\left[\text{because } c = \left[\frac{E}{\rho}\right]^{\frac{1}{2}}\right]$

Reynolds number is a measure of the ratio of inertial to viscous forces and is a useful parameter ensuring equivalence of energy losses between model and prototype.

Froude number indicates the ratio of inertial force to gravitational force, and the Weber and Mach numbers are similar ratios involving the surface tension and elastic forces respectively.

The working fluid in a ship tank in which model ships are tested is the same as the working fluid in the prototype system (the sea) although probably not saline. This implies that equivalence of all four of the above parameters between model and prototype will not be possible. Gravity waves on water are principally characterised by the Froude number, so the models which are discussed in this paper will be constructed according to Froude's scaling laws. Very little energy is lost from waves propagating over the length of a ship tank, so the absence of matching of Reynolds numbers should not be significant. Similarly, elasticity plays little part in the behaviour of surface waves on water. At very short wavelengths (of the order of millimetres), surface tension effects begin to exert some control over the waves. These very short waves are known as capillary waves, and the need to avoid them if Froude scaling has been applied places limits on the range of wavelengths which can be modelled and the linear scale ratio to which the model can be constructed. Failing to observe this restriction would cause other practical problems; for instance gravity waves can be measured with surface-piercing probes whereas capiliary waves obviously cannot.

Relationships between model and prototype can be deduced in the following manner:

(a) Linear scale ratio = $\frac{d_m}{d_p}$ (typical value is $\frac{1}{20}$)

(b) Froude number equivalence $F_m = F_p$

$$\text{therefore } \frac{V^2_m}{gd_m} = \frac{V^2_p}{gd_p}$$

$$\frac{V^2_m}{V^2_p} = \frac{d_m}{d_p} \quad - (1) \quad \text{therefore } \frac{V_m}{V_p} = \sqrt{\frac{d_m}{d_p}}$$

(c) $V = \frac{d}{t}$

$$\text{therefore } \frac{d^2_m}{t^2_m} \cdot \frac{t^2_p}{d^2_p} = \frac{d_m}{d_p} \text{ (by substitution in (1)).}$$

$$\frac{t_{p^2}}{t_{m^2}} \cdot \frac{d_m{}^2}{d_p{}^2} = \frac{d_m}{d_p}$$

$$\text{therefore } \frac{d_m}{d_p} = \left[\frac{t_m}{t_p}\right]^2 \qquad \text{therefore } \frac{t_m}{t_p} = \sqrt{\frac{d_m}{d_p}}$$

The principles described above are used in modelling a wide range of hydraulic phenomena in both civil engineering and marine technology. This paper concentrates on the modelling of sea-states in towing tanks so that the seakeeping performance of ships can be studied using laboratory scale models.

The testing of ships is rather more difficult than the testing of civil engineering structures, because structures generally remain in place whereas ships translate relative to the sea. The objective of the paper is to describe in non-mathematical terms the behaviour of waves in model testing tanks and to show how this behaviour restricts the experiments which can be done, and dictates the methods which must be employed.

This is a subject which can easily be dominated by difficult mathematics but this paper concentrates on qualitative descriptions and the solution of practical problems. Wherever possible, approximate results are derived by simple methods. When these methods do not yield results of adequate precision, then a statement of the results of more accurate computation is given, with an attempt at providing a physical justification. Wherever illustrations of actual ship tank performance are given, they relate to No 1 Ship Tank at ARE (Haslar). (See Figure 1.1).

Sections 2-6 describe the behaviour of regular waves in a ship tank. Regular waves are only useful for testing linear phenomena when it can be assumed that the response to a number of spectral lines is the sum of the responses to each (regular) line on its own; and when increasing or decreasing the amplitude of the waves results in an exactly proportional increase in response. The results of such tests

are usually expressed as transfer functions or cross-spectral densities. Non-linear phenomena must be tested in random or pseudo-random waves and the later sections extend what has been said about regular waves to cover the behaviour of irregular ones.

2. REGULAR WAVES

Regular waves are usually described by equations developed from the theory of Airy (1) or Stokes (2) in the middle of the 19th century. The Airy theory essentially applies to gravity waves of infinitessimal amplitude whereas Stokes' work extended to finite amplitude waves. The surface profile of a very small wave is sinusoidal, and hence the Airy equations are much easier to use. In practice they also produce results which are adequate for most engineering purposes, although Stokes' results will be more accurate for large waves in depths which are small compared with the wavelength. Most ship tanks are deep compared with the wavelengths which can be generated in them.

2.1. Airy Expressions

Refering to Figure (2.1) the surface form of the regular wave is given by:

$$z = (\tfrac{1}{2} H) \cos 2\pi \left[\frac{x}{\lambda} - \frac{t}{T}\right]$$

Note that this implies that the wave field is of infinite extent in both time (t) and distance (x).

The celerity (ie the speed of propagation of the waves) is given by:

$$C^2 = \left[\frac{g\lambda}{2\pi}\right] \tanh \left[\frac{2\pi D}{\lambda}\right]$$

which reduces to:

$$C_o^2 = \left[\frac{g\lambda o}{2\pi}\right] \quad \text{in deep water (see Figure 2.2).}$$

In practice, the water can be considered as being deep if:

$$\frac{D}{\lambda} > 0.5.$$

In very shallow water, the celerity expression reduces to:

$$C^2 = gD.$$

On the assumption that the wave period is invariate, it is now possible to deduce an expression which indicates how the wavelength varies with depth, using the relationship $c = \lambda/T$.

$$\lambda = \left[\frac{gT^2}{2\pi}\right] \tanh \left[\frac{2\pi D}{\lambda}\right]$$

The expression requires an iterative method of solution, preferably with the assistance of a personal computer.

2.2. Orbital Motion

As a wave passes, the elements of water below it travel in closed paths, which are circular near the surface. The diameter of the circular path taken by an element which was initially at the surface is exactly equal to the waveheight H. In very deep water, the diameter of the paths reduces with depth, but the paths remain circular. In shallow water, elements of water move in generally elliptical orbits, with the vertical axis of the ellipse reducing to negligible size at the bottom.

The horizonal and vertical displacements of the element are given by:

$$\xi = -\frac{1}{2} H \frac{\cosh \left[\frac{2\pi(D+z)}{\lambda}\right]}{\sinh \left[\frac{2\pi D}{\lambda}\right]} \sin 2\pi \left[\frac{x}{\lambda} - \frac{t}{T}\right]$$

$$\eta = \frac{1}{2} H \frac{\sinh \left[\frac{2\pi(D+z)}{\lambda}\right]}{\sinh \left[\frac{2\pi D}{\lambda}\right]} \cos 2\pi \left[\frac{x}{\lambda} - \frac{t}{T}\right]$$

where z in the initial distance between the element and the still water surface, and is negative for elements which are initially below the surface.

An example of the orbits of elementary particles of water under a wave is given in Figure 2.3. The orbital velocity and acceleration components can be computed by differentiation of the above equations with respect to time.

2.3 Stokes expressions

The Stokes expressions do not assume that the wave has a very small amplitude and hence do not result in a sinusoidal surface form. Finite amplitude waves are characterised by long troughs and sharp crests as illustrated in Figure 2.4. The surface form therefore includes harmonics of the fundamental sinewave which are bound to the fundamental in phase, ie they do not travel at the celerity which would be expected if the harmonic was a free wave of the same period.

Replacing $2\pi \left[\frac{x}{\lambda} - \frac{t}{T}\right]$ by θ, the Stokes equations, to a third order of approximation, for the surface form of the wave are:

$$z = a \cos \theta + \left[\frac{\pi}{\lambda}\right] a^2 \cdot f_2 \left[\frac{D}{\lambda}\right] \cdot \cos 2\theta + \left[\frac{\pi}{\lambda}\right]^2 a^3 \cdot f_3 \left[\frac{D}{\lambda}\right] \cdot \cos 3\theta$$

$$\text{where } f_2\left[\frac{D}{\lambda}\right] = \frac{\cosh\left[\frac{2\pi D}{\lambda}\right] \cdot \left[\cosh\frac{4\pi D}{\lambda} + 2\right]}{2\left[\sinh\frac{2\pi D}{\lambda}\right]^3}$$

$$\text{and} \quad f_3\left[\frac{D}{\lambda}\right] = \frac{3}{16} \cdot \frac{8\left[\cosh\frac{2\pi D}{\lambda}\right]^6 + 1}{\left[\sinh\frac{2\pi D}{\lambda}\right]^6}$$

The relationship between the amplitude of the fundamental component (a) and the waveheight (H) is given by:

$$H = 2a + 2\left[\frac{\pi}{\lambda}\right]^2 \cdot a^3 \cdot f_3\left[\frac{D}{\lambda}\right]$$

The celerity is given by:

$$C^2 = \frac{g\lambda}{2\pi}\tanh\frac{2\pi D}{\lambda}\left[1 + \left[\frac{2\pi a}{\lambda}\right]^2 \cdot \frac{\cosh\frac{8\pi D}{\lambda} + 8}{8\left[\sinh\frac{2\pi D}{\lambda}\right]^4}\right]$$

The term in brackets may be considered as a correction factor applied to the results of the simpler Airy expressions.

2.4 Particle Trajectory

Since the surface form is not now sinusoidal, one would expect the orbital velocity of an element of water to vary depending on the phase of the wave passing over it. The Stokes expressions for particle velocity are:

$$\dot{\xi} = C\,(U_1 \cos\theta + U_2 \cos 2\theta + U_3 \cos 3\theta)$$

$$\dot{\eta} = C\,(V_1 \sin\theta + V_2 \sin 2\theta + V_3 \sin 3\theta)$$

$$\text{where } U_1 = \frac{2\pi a}{\lambda} \cdot \frac{1}{\sinh\frac{2\pi D}{\lambda}} \cdot \cosh\frac{2\pi S}{\lambda}$$

$$V_1 = \frac{2\pi a}{\lambda} \cdot \frac{1}{\sinh\frac{2\pi D}{\lambda}} \cdot \sinh\frac{2\pi S}{\lambda}$$

$$U_2 = \frac{3}{4}\left[\frac{2\pi a}{\lambda}\right]^2 \frac{1}{\left[\sinh\frac{2\pi D}{\lambda}\right]^4}\cosh\frac{4\pi S}{\lambda}$$

$$V_2 = \frac{3}{4}\left[\frac{2\pi a}{\lambda}\right]^2 \frac{1}{\left[\sinh\frac{2\pi D}{\lambda}\right]^4}\sinh\frac{4\pi S}{\lambda}$$

$$U_3 = \frac{3}{64}\left[\frac{2\pi a}{\lambda}\right]^3 \left[\frac{11 - 2\cosh\frac{4\pi D}{\lambda}}{\left[\sinh\frac{2\pi D}{\lambda}\right]^7}\right]\cosh\frac{6\pi S}{\lambda}$$

$$V_3 = \frac{3}{64}\left[\frac{2\pi a}{\lambda}\right]^3 \left[\frac{11 - 2\cosh\frac{4\pi D}{\lambda}}{\left[\sinh\frac{2\pi D}{\lambda}\right]^7}\right]\sinh\frac{6\pi S}{\lambda}$$

where S is the instantaneous elevation of the element above the bottom, ie $S = D + z + \eta$.

The orbital trajectory can be deduced by calculating the velocity at small increments of phase and plotting a vector diagram similar to the example in Figure 2.5. The trajectory will not generally be circular, and there may be an overall translation of the element in the direction of propagation of the waves. This translation of water occurs near the surface, and in a closed tank must be balanced by a reverse flow along the bottom. A circulation of water will therefore develop if large waves are generated for a considerable length of time, and this circulation will persist for a long time after the wave generator is stopped.

2.5. Capilliary Waves

It was mentioned in section 1 that the principles which make model testing possible break down if the gravitational forces do not dominate the behaviour of both model and prototype. The most likely error is that waves in the model may be affected or controlled by surface tension rather than gravity.

In section 2.1 the expression

$$C_o^2 = \frac{g\lambda o}{2\pi}$$

was derived for the celerity (wave speed) of gravity waves on deep water. This expression can be extended to include the effects of surface tension, and becomes

$$C^2 = \frac{\lambda_o g}{2\pi} + \frac{2\pi T}{\rho\lambda_o}$$

The solution of this equation is not straightforward. However, as can be seen from Figure 2.2, the assumption that waves are controlled by gravity is valid for wavelengths greater than about 0.2 metres.

3. PROPAGATION OF REGULAR WAVES

The results given in section 2 apply to continuous regular waves. In the ship tank, the wave train is finite in both time and length, and hence we must know more about the behaviour of finite groups of waves.

3.1 Wave Energy

Firstly, we need an estimate of the energy which is present in the wave train. Assuming the Airy description of the waves can be applied, an expression can be deduced for the mean potential energy per unit surface area without recourse to any complicated mathematics.

Referring to Figure 3.1, and section 2.1 the surface form is given by:

$$z = \frac{1}{2} H \cos 2\pi \left[\frac{x}{\lambda} - \frac{t}{T}\right]$$

When $t = 0$ the instantaneous surface profile is

$$z = \frac{1}{2} H \cos 2\pi \left[\frac{x}{\lambda}\right]$$

The mass of the element z, δx is $m = \rho z \delta x$ and its mean distance from the still water level is $\frac{1}{2} z$.

Hence the potential energy, per unit width of channel, of the element is

$$P E = \frac{1}{2} g \rho z^2 \delta x$$

The potential energy per unit wavelength is therefore

$$PE = \frac{1}{2} \rho g \int_{x=0}^{x=\lambda} \left[\frac{1}{2} H \cos 2\pi \left[\frac{x}{\lambda}\right]\right]^2 \delta x$$

$$PE = \frac{H^2 \rho g}{8} \int_0^{\lambda} \cos^2 2\pi \left[\frac{x}{\lambda}\right] \delta x$$

$$PE = \frac{H^2 \rho g}{8} \left[\frac{1}{2} x + \frac{1}{4} \sin 2x\right]_0^{\lambda}$$

$$PE = \frac{H^2 \rho g \lambda}{16}$$

The mean PE per unit surface area is therefore $\frac{\rho g H^2}{16}$.

The Kinetic energy is rather more difficult, because it involves integrating

$$\left[\left[\dot{\xi}\right]^2 + \left[\dot{\eta}\right]^2\right]$$

over z and x, where ξ and x are given by the expressions of Section 2.2. It is not unreasonable to accept the result that the mean kinetic energy is equal to the mean potential energy per unit surface area. (Proof of this is given in Appendix 1.)

The total energy per unit surface area is therefore

$$\frac{H^2 \rho g}{8} \text{ Joules/m}^2$$

3.2 Energy Propagation

The instantaneous rate of doing work is given by

$$\int_0^D p\,\dot{\xi}\,dz$$

where p is the pressure.

The average rate of transmission of energy is

$$W = \int_0^\lambda \frac{\int_0^D p\dot{\xi}\,dz}{\lambda}\,dx$$

Which yields the result

$$W = \frac{\rho g H^2 C}{8}\left[\frac{1}{2} + \frac{\frac{2\Pi D}{\lambda}}{\sinh\frac{4\Pi D}{\lambda}}\right]$$

This can be re-written as

$$W = \frac{\rho g H^2}{8} \cdot V$$

$$\text{where } V = C\left[\frac{1}{2} + \frac{\frac{2\pi D}{\lambda}}{\sinh \frac{4\pi D}{\lambda}}\right]$$

V, which is the velocity at which energy is transmitted, is the group velocity of the waves.

In deep water, where D/λ is large, this expression reduces to $V = \frac{1}{2} C$.

In deep water, the total wave energy propagates at a group velocity which is half of the celerity of the waves. There is, however, an alternative way of viewing the result. This is to say that no kinetic energy actually propagates because elementary water particles travel in closed orbits without translation, and hence the result indicates that only the potential energy is propagating. If this is the case, the speed of propagation is equal to the celerity of the waves.

This is actually a more productive view to take, because it leads to a physical picture which closely represents the way in which waves propagate in a tank. Let us assume that we have been able to generate three waves of equal amplitudes in the tank, as illustrated, in Figure 3.2(a), which can be considered as a snapshot of the water surface at a time t = 0. (For the present we will overlook the extreme difficulty of actually doing this.) If the potential energy is half of the total, and travels at the celerity, then the situation at time t = T will be as shown in 3.2(b). Half the energy of the first wave has propagated forwards by one wavelength, and the last wave has lost half of its energy. The two intermediate waves have lost as much energy forwards as they have gained from behind, and hence their amplitude is unchanged. Extending this process to time t = 2T, yields Figure 3.2(c),and so on. Examination of Figure 3.2shows that the leading edge of the surface disturbance travels at the celerity, but that the middle of the wave group travels at half the celerity, and it is now obvious why this is called the group velocity. Figure 3.3 shows the relationship between group velocity and celerity for different ratios of depth to wavelength.

Figure 3.3 therefore shows something of the behaviour of a finite group of waves, and is very important because it leads to one of the principal difficulties in using a ship tank. It shows that we cannot fill the tank with a regular wavetrain in which all of the waves have the same amplitude at any given time.

3.3 Initiating the Wavetrain

The last section started with the assumption that a finite group of regular waves of equal height could be produced and then predicted how they would propagate. Now that we know something of how they would propagate, it is possible to think backwards and wonder how they might have been produced in the first place. It is clear that this would not have been a trivial problem.

Waves are generated from the end of the ship tank where the wavemaker is sited, so the wavegroup would be the spatial distribution of water level at an instant in time resulting from a temporal distribution

generated at some position in space. An attempt to calculate backwards from the required wave group to the necessary input signal is fraught with problems because it appears that the first wave to be generated must be very large if it is to have the correct amplitude by the time the rest of the group has been generated. Such a violent commencement of activity at the wavemaker will introduce other frequencies as well as the fundamental frequency of the regular waves. Since these frequencies travel at their own celerities, interference will occur in the tank between the various frequency components associated with the wavemaker start-up. ARE(Haslar) commissioned a study of this problem, and a report (4) has now been received. This shows that the envelope of waveheights passing a point in the tank as a result of suddenly applying a constant amplitude sinewave at the wavemaker is represented by the magnitude of a Cornu Spiral, and this is illustrated in Figure 3.4.

The horizontal axis of Figure 3.4 is in units of $t\sqrt{\frac{g}{4\pi x}}$ implying that the envelope of the waves which pass a point in the tank is dependent only on the separation between that point and the wavemaker, and is independent of the wave period. An initial overshoot of about 17½ per cent above the required waveheight is predicted, followed by lightly damped oscillations about the required waveheight. The horizontal axis zero corresponds to the group delay on the waves travelling from wavemaker to measuring point.

Having considered what happens when the wavemaker signal is 'suddenly' switched on, the reference considers the effect of applying a gaussian window to the wavemaker input signal. (The type of window was chosen for ease of analysis rather than optimum results).

The sinusoidal demand signal is passed through a network having time-varying gain according to the equation

$$G(t) = \frac{1}{\sigma\sqrt{2\pi}} \int_0^t e^{-\frac{\tau^2}{2\sigma^2}} \, \partial\tau$$

where σ has been chosen to be $\sqrt{\frac{2x}{g}}$, x being the distance along the tank where we are going to measure or use the waves. Taking, as an example, x = 100 m gives the wavemaker input curve at the top of Figure 3.5, and the resulting history of wave amplitudes at x = 100 m, which is shown at the bottom of Figure 3.5. The improvement is obvious, but it must be remembered that this improvement is obtained at a predetermined place in the tank. As waves propagate beyond this point, the benefit of the windowed input signal reduces, so that (for example) waves reflected back into the tank from the beach will probably show an oscillatory overshoot somewhere between the characteristics of Figure 3.5 and the one of Figure 3.4.

3.4 Breaking Waves in the Tank

It will be shown later that the disturbance near the wavemaker consists of two parts, a local one which decays over a horizontal distance equivalent to about four depths of the tank, and the propagating one which results in the propagating waves. We expect, therefore, that as a result of sinusoidal excitation of the wavemaker, a stable regular wave will develop from about 10 m into the tank and propagate without any significant change until it reaches the beach. Over a wide range of waveheights and frequencies, this expectation will be satisfied, but there are some conditions under which it will not.

Firstly, we may think that energy will be lost from the waves as a result of friction between the moving water particles and the tank. The tank is deep enough for bottom friction to be insignificant (otherwise we would not be able to use the deep water approximation of the wave equations). As an example, waves of 1 sec period and 0.1 m peak-peak waveheight transmit approximately 10 W of power per metre width of tank. Absorption at the bottom of the tank is calculated to be of the order $(3 \rightarrow 30) \times 10^{-13}$ watts per square metre. If significant amounts of energy were being extracted from the waves at the walls, we would measure changes in waveheights and/or group velocity as the waves propagate along the tank. For small waves at long wavelengths, such changes cannot be detected. For larger waves, or shorter wavelengths, big changes, can be detected, but these are not due to absorption.

Waves will break in the tank if the maximum value of the horizontal component of orbital velocity exceeds the wavespeed, because this implies that the wave crest is travelling faster than the rest of the wave. An estimate of the conditions under which this problem will occur can therefore be made:

In deep water $\quad Co^2 = \frac{g\lambda}{2\pi}$

At the surface, $\quad \left[\frac{\partial \xi}{\partial t}\right]_{max} = \frac{\pi H}{T} \left[\frac{\cosh \frac{2\pi D}{\lambda}}{\sinh \frac{2\pi D}{\lambda}}\right]$

if $d > \frac{1}{2} \lambda$, then $\tanh \frac{2\pi D}{\lambda} \approx 1$

therefore $\left[\frac{\partial \xi}{\partial t}\right]_{max} = \frac{\pi H}{T} = \frac{\pi H C}{\lambda}$

Hence $\left[\frac{\partial \xi}{\partial t}\right]_{max} > Co$ when

$$\frac{\pi^2 H^2}{\lambda^2} \left[\frac{g\lambda}{2\pi}\right] > \frac{g\lambda}{2\pi}$$

ie when $\frac{H^2}{\lambda^2} > \frac{1}{\Pi^2}$

or $\frac{H}{\lambda} > 0.3$

This estimate is inaccurate because Airy's assumptions of small waveheight, long wavelength, and sinusoidal surface profile are very far from the conditions which exist in a wave which is about to break in deep water.

It has been shown (5) that the limiting shape for the angular wavecrests predicted by Stokes' theory has an included angle at the crest of 120 degrees, and that this corresponds to:

$$\frac{H}{\lambda} = 0.142$$

Any attempt to produce waves which exceed this limiting steepness will result in breaking waves throughout the ship tank. Fortunately, it is rarely necessary to test models in such large regular waves.

For some wave steepnesses which are within this limiting range, we find that stable regular waves form about four depths from the wavemaker, propagate for perhaps 20 wavelengths down the tank, and then disintegrate into an irregular mess of breaking waves. When the wavelength is short enough, there is a subjective impression that the region over which this mess extends is finite and that regular waves begin to re-form on the far side, near the beach. This phenomenon is analysed in Reference 6, which suggests that it is part of the mechanism by which real seas develop from short, small amplitude ripples to long, large amplitude, swells. We will return to this subject later when we discuss random seas. For the moment, however, we are interested only in the effect on regular waves.

Figure 3.6 shows what is really happening when a regular wavetrain disintegrates. The figure shows the energy density spectrum measured near the wavemaker, in the region of the visible disintegration about halfway along the tank, and in the region where some subjective impression of regularity is returning near the beach at the far end of the tank from the wavemaker. The input wavetrain has an amplitude of 0.26 metres peak to peak and a period of 1 sec. As can be seen the spectrum is narrow (narrower than the resolution of our measurement) and the amplitude of the Stokes' harmonic frequencies is very low. As the wavetrain disintegrates, sidebands appear at ± 0.83 Hz relative to the fundamental. (This figure corresponds exactly to the prediction of Reference 6 for this waveheight and period.) Near the beach, the lower sideband has nearly the same energy as remains in the original fundamental, and one might speculate that, eventually, most of the energy from the original regular wave would be transfered into a new regular wave at a lower frequency. This would account for the subjective impression that regular waves are re-forming in the tank, and throws some light on the way in which sea states develop with time and fetch under the influence of wind.

4. GENERATING WAVES

4.1 Wavemakers

Waves are generated in tanks by the physical displacement of a plunger, wedge, piston or hinged flap; or by the application of a variable air pressure to part of the water surface. Figure 4.1 shows the various types of wavemaker which are in use.

In principle, there is little to choose between the first four types in terms of their ability to make waves. The choice usually results from practical considerations such as:

a. Absence of waves behind the wave generator.

b. Linearity.

c. Minimal buoyancy force.

d. Ease of movement or installation.

e. Magnitude of the reaction force against the surrounding structure of the tank.

f. Mechanical complexity.

g. Installation cost.

Pneumatic machines are rarely used. They have the particular advantage of having no moving parts in the water, and the ability to distribute the wavemaking "force" over a very wide wavefront. Their principal disadvantage is that they lack "stiffness" because of the high compressibility of air, resulting in low natural frequencies and poor control of the waves. The machine is therefore most suited to generating narrow-band, long period, long crested, low amplitude, regular waves. Modern requirements tend towards short-crested random waves. In spite of its disadvantages, the advantages of the pneumatic wavemaker are significant ones, and it may become popular again in the future.

4.2 Wavemaker Calibration

When a mechanical wavemaker is driven with a sinusoidal displacement, then stable regular waves develop within about four depths ($x = 4D$) from the wavemaker, and propagate along the tank.

The region within four depths of the wavemaker includes a local disturbance which decays exponentially with distance and should not be included in any test run. It is desirable that the vertical distribution of the horizontal component of velocity of the front face of the wavemaker should closely match the horizontal component of particle velocity in the waves, but clearly this is not possible over any reasonable range of wave frequencies and amplitudes. Excess wavemaker movement at depth results in high reactive forces and greater local disturbance near the wavemaker but contributes little to the wave amplitude further along the tank. An excess of this stroke

can also result in the establishment of standing waves across the face of the wavemaker, perpendicular to the direction of propagation of the travelling waves. The water particles in the standing wave oscillate at half the wavemaker frequency.

By postulating a velocity potential which satisfies surface and bottom conditions and gives a wave travelling away from the wavemaker as $x \to \infty$, and equating the horizontal velocities of the paddle with those of adjacent water particles it is possible to predict the relationship between wavemaker stroke and the resulting waveheight.

It is also possible to predict the force necessary to actuate the wavemaker. This force consits of a dissipative component, in phase with the wavemaker velocity and obviously connected with the propagating wave energy; and a reactive component, connected with the local disturbance near the wavemaker, and in phase with the acceleration.

Reference (3) presents design curves calculated in this way and includes further references to the theory on which the method is based.

The design curves predict small values of $\frac{\text{waveheight}}{\text{stroke}}$ (H/s) for long wave periods (T), rising to a value close to H/S = 2 when $gT^2 = D$ and remaining at this value for shorter wave periods. Usually, however, the measured calibration curves fall off at high frequencies, and curves similar to Figure 4.2 are obtained. The design curves predict (H/S) where s is the horizontal component of the stroke of the wavemaker, but Figure 4.2, which is the actual calibration of the wavemaker on No 1 Ship Tank at Haslar is plotted with reference to the vertical component of stroke. The machine is a plunger with wedge angles of 25 degrees and 15 degrees. The machine produces larger waves than the theory predicts, presumably because the theory does not account for the variation in displacement with vertical position.

The plunger is actuated by a servo control system - in this case a hydraulic one. It is prudent to limit the forces and accelerations which might be experienced by the wavemaker; particularly at high frequencies where small strokes would produce large waves, but the maximum waveheight is limited by wave breaking. This is usually achieved by restricting the bandwidth of the servo, and possibly by the use of a low pass filter in the input signal line. Taking account of the servo and any filter, it is possible to predict (and measure) a wavemaker calibration in terms of waveheight per volt of input signal versus frequency. Figure 4.3 is the measured calibration of the machine.

4.3 Performance Limits

Having obtained or predicted the wavemaker calibrations, we are in a position to predict the limiting performance of the installation for regular waves. The prediction for No 1 Ship Tank is given as Figure 4.4. As can be seen, the maximum waveheight at low frequencies will be limited by the stroke of the wavemaker. At high frequencies it will be limited because the waves will reach unstable steepness and break. In some installations, other limiting curves may also be

significant - for instance limited actuator force or frequency response of the servo might limit the maximum waveheight, although this is not the case for our machine.

The hatched line shows the region of the graph where the regular waves might disintegrate as a result of the Benjamin-Feir instability. It will be recalled from the previous section that the waves travel perhaps 20 wavelengths along the tank before disintegrating, so the importance of this limiting line will depend on the length of the tank.

Figure 4.5 is the measured performance limit graph for No 1 Ship Tank. The stroke limit was predicted fairly closely in the previous graph, but the wall height limit was overlooked. This is clearly an important limit if the experimenter wants to keep his socks dry! The measured breaking wave limit is lower than predicted because the measurements incorporate observations of Benjamin-Feir disintegration as well as immediate breaking of waves near the wavemaker.

5. ABSORBING WAVES

So far, we have discussed the way in which waves propagate along the tank and the method by which they are generated. We must also take steps to absorb waves when they reach the far end of the tank from the wavemaker, to avoid contamination of the generated wavetrain by another wavetrain travelling in the opposite direction. It is also possible that the model under test may reflect a significant amount of wave energy back towards the wavemaker, which is very likely to be a good reflector. Energy reflected from the model at the beginning of a test run may be reflected back from the wavemaker, and interfere with the generated waves, before the test run ends.

Most existing ship tanks are fitted with passive beaches to absorb waves at the far end of the tank, and have no equipment to deal with reflections from the wavemaker.

5.1 Passive Beach Performance

One of the constraints on the design of a ship tank beach is that part of it must be removable so that models can be rigged on to the towing carriage in a dock at the end of the tank, and then brought out through the position of the beach, which is then replaced prior to testing. Simple, passive, beaches are therefore preferred. They usually consist of a sloping, slatted surface extending through the water surface, but not to the bottom of the tank. This is fairly easy to remove, and is often made from materials which have nearly neutral buoyancy so that it can be simply floated to one side as models are brought out of the dock. The design objective is to minimise the reflection coefficient over the full range of waveheights and periods. Variables which may be adjusted to achieve this include slat size and spacing, slope, length, and intercept with the still water level. Actual beaches, however, rarely seem to have been designed at all. They are often a collection of various surfaces and structures, both curved and plane, built up as a succession of 'ad hoc' improvements to what was already there. The beach structure is therefore complicated in direct proportion to the age of the tank and in an old tank it is

probably possible to remove most of the beach without causing much change of performance.

In regular waves, low reflection coefficients are achieved by ensuring that waves break as they run up the beach. If the beach is steep, this may not happen because the wave does not travel a sufficient distance on the beach to break, and very high reflection coefficients result. If the waves are small, but the beach is long, they may surge on and off the beach without actually breaking. This results in higher reflection coefficients than if the wave breaks.

5.2 Passive Beach Design

It is necessary to estimate the waveheight at breaking and the wave run-up on the beach in order to ensure that the tank walls and beach are high enough, and to estimate the depth of the beach at the point where waves will break in order to ensure that the beach extends for a sufficient distance below the still water surface.

An estimate of the waveheight and beach depth at breaking can be made by using the results of experimental work by Iversen (7) and the Airy wave theory.

Wave energy per unit surface area = $\frac{\rho g H^2}{8}$

In deep water, this energy propagates at a group velocity, V_o, equal to one half of the celerity C_o.

Therefore power per unit width of wavefront = $\frac{\rho g H_o C_o}{16}$

In shallow water, the group velocity is equal to the celerity so

$$V_B = C_B = \sqrt{gD_B}$$

and the power per unit width of wavefront $= \frac{\rho g H^2_B \sqrt{gD_B}}{8}$

If no power is dissipated as the wave moves from deep water to shallow water, then

$$\frac{\rho g H_o^2 C_o}{16} = \frac{\rho g H_B^2 \sqrt{gD_B}}{8}$$

$$\text{therefore } \left[\frac{H_B}{H_o}\right]^2 = \frac{C_o}{2\sqrt{gD_B}}$$

$$\text{ie } \left[\frac{H_B}{H_o}\right]^4 = \frac{C_o^2}{4gD_B}$$

Iversen's data shows average Values for $\frac{d_B}{H_B}$ of about 1.0 for 1:10 beach slopes and about 1.2 for 1:50 beach slopes. Civil Engineers usually

assume a value of 1.28 for naturally occuring beaches, but ship tank beaches need to be short and are generally steep.

Assuming $\frac{D_B}{H_b} = 1$

then $\frac{H_B^5}{Ho^4} = \frac{C_o^2}{4g}$

and since $C_o = \sqrt{\frac{g\lambda_o}{2\pi}}$

then $\frac{H_B^5}{Ho^4} = \frac{\lambda o}{8\pi}$

or $\left[\frac{H_B}{H_o}\right]^5 = \frac{1}{8\pi}\left[\frac{\lambda_o}{H_o}\right]$

where λo and Ho are the wavelength and height in the tank and (H_B/Ho) is the ratio of breaker height on the beach to waveheight in the tank. From the method used to derive this formula, it should only be expected to provide an indication of the height and depth of waves breaking on a beach. Michells formula, (Reference 5) which is known to be in reasonable agreement with measured data, takes the limiting wave steepness in deep water, $H_o/\lambda o = 0.142$ (mentioned in Section 3) and corrects it by a factor relating the shallow water celerity to the deep water celerity so that

$$\frac{H_B}{\lambda_B} = 0.142 \tanh \frac{2\pi D_B}{\lambda_B}$$

The worst case in the ship tank is for waves at a period of 2.08 sec. The wavelength in the tank is 6.6 m and the maximum waveheight which produced is 0.26 m. The simple formula suggests that these waves will hardly increase in amplitude before breaking on the beach, which is not unreasonable because the waves are not far short of breaking in deep water. Tracking the wavelength and waveheight as the wave progresses from deep water to shallow water (a more tedious method) and applying Michells formula suggests that they will break at an amplitude of 0.326 m over a depth of 0.42 m at a wavelength of just over 6 m. To prevent water overtopping the tank sides the walls need to be raised by about 3½ cm along either side of the beach. We also need to know if water can overtop the beach slope. Run-up is defined as the vertical distance above the still water level that the wave will reach on the sloping beach. The run-up depends on the wavelength, the depth of the foot of the beach, the slope and roughness of the beach and the deep water waveheight. The results of experiments (8) are therefore difficult to present, but for our purpose we are only interested in maximum values.

On a smooth beach of any slope, the maximum run-up will occur at the lowest value of H_{o/T^2} where Ho is the waveheight in the tank and T is its period. From the measured performance limit graph we find that, for our ship tank

$$\left[\frac{H_o}{T^2}\right]_{min} = 0.17 \text{ (at 1.1 Hz app)}$$

Figure 5.1 is a graph, prepared from experiment results, of the maximum run-up on different slopes for this value of (H_o/T^2). It should be noted that the graph is only valid if the depth of the foot of the beach is greater than Ho. If this is not the case, and the slope is greater than about 1:5, the waves will not have time to break on the beach. The run-up will then be independent of beach slope, and the reflection coefficient will be high. The maximum possible run-up is seen to be 0.28 m above the still water level, on a beach slope of 1:2. The slope of the existing beach is actually 1:3 and it is obvious that this could be regularly over-topped. If we assume that the tank walls can be raised by 3½ cm on either side of the beach to contain the maximum breaking waveheight, then we will have a freeboard of 0.165 m, limiting the maximum allowable beach slope to 1:5.

At this stage we can summarise the constraints on the beach design.

a. The bottom of the beach must be deeper than the maximum peak-peak waveheight (0.26 m).

b. If the beach is to break waves with the maximum value of breaking waveheight, the bottom of the beach must be deeper than 0.42 m.

c. The walls either side of the beach, and the crest of the beach should be 3.5 cm higher than the walls over the rest of the tank's length.

d. The beach should be as short as possible for mobility.

e. The slope should not be steeper than 1:6.

The constraints combine to give a minimum plan length for the beach of 3.5 m.

5.3 Measuring Reflection Coefficient

It is not easy to measure the beach reflection coefficient, even in regular waves. Three methods have been used, and we have found that all three are necessary if measurements are to be made over a wide range of frequencies and waveheights. The major problems are the difficulty of ensuring a constant incident wave on the beach during measurements, and the need to make measurements using regular waves which are far from the 'Airy' sinusoidal surface profile.

Method 1

Generate a finite group of regular waves and measure the entire group, as it passes a point about 2/3 of the way along the tank, in both the incident and the reflected directions. This method is only useful over a very limited range, because it is necessary to ensure that the incident group can be distinguished from the reflected group, and that the reflected group is not contaminated by a further reflection from

the wavemaker. Also, the shape of the group changes as it propagates so it is necessary to measure the total energy in the group before and after reflection and deduce the reflection coefficient from this. Finally, the measurement is not made at a constant wave amplitude, so any amplitude dependence is obscured.

Method 2

The wavemaker is operated at a constant stroke and frequency, until conditions are stabilised in the tank. A waveprobe is mounted on the towing carriage, which is run very slowly through the standing wave which forms, near the beach. This results in a record like Figure 5.2, in which the standing wave is clearly visible. Taking Hmax and Hmin as the maximum and minimum amplitudes of the envelope of this record, then

$$\text{Reflection coefficient} = \frac{H \text{ reflected}}{H \text{ incident}} = \frac{Hmax - Hmin}{Hmax + Hmin}$$

This method assumes that the incident waveheight is independent of both time and position in the tank. As was shown in Section 3, time independence may require that the measurement is made a very long time after starting the wavemaker, but position independence requires that the measurement be unaffected by re-reflection (of the wave reflected from the beach) by the wavemaker. The method is, like Method 1, rather limited in its range of application. The figure shows a 'good' result, but frequently no standing wave can be discerned, although the measured wave amplitude is far from constant.

It should be noted that, in principle, it is not necessary to traverse the standing waves with a slowly moving waveprobe. The standing wavelength is predictable so two measurements made using stationary probes are sufficient to define the result. Methods of measuring reflection coefficient in irregular or random waves use a number of waveprobes in an extension of the technique which has just been described.

Method 3

As before waves are generated until their amplitude has stabilised, but this time the waveprobe moves at the calculated celerity of the waves. When the probe is moving towards the beach, the incident wave signal is shifted to zero frequency and the reflected wave signal appears at twice the fundamental frequency of the waves which are being generated. When the probe is moving away from the beach, the incident waves appear doubled in frequency and the reflected waves shift to zero frequency. Spatial dependence of either incident or reflected waves is immediately obvious, although several 'runs' may be necessary to eliminate the possibility of temporal variations. The method can cope with very non-sinusoidal waveforms provided that all harmonic components are locked to the celerity of the fundamental and do not propagate as free waves. A typical record from this method is shown as Figure 5.3 in which the results are so clear that a rule and calculator are adequate for analysis. In more difficult cases (eg if some other frequencies are present) the results can be analysed by computing the spectral density functions for each record and comparing them.

In general, hand analysis is possible if the wave probe speed is exactly equal to the wave clerity so that one of the signals is shifted to zero frequency. Otherwise, spectral analysis methods must be employed. The lower part of Figure 5.4 shows an example of a record which is difficult to analyse by either method. Apparently an incident wave with an easily distinguished dominant frequency has been reflected as a wave with several frequencies present. The total energy in the incident and reflected spectra can be compared, and if necessary expressed as an equivalent reflection coefficient. Care must be taken, however, to check that the two spectra do indeed represent incident and reflected waves, and not the contribution of spurious other waves or harmonics of the incident wave in the tank. Repeating the test at different towing speeds will give some indication of this.

5.4 Reflection Coefficient of Existing Beach

The beach in Haslar No 1 Ship Tank before December 1988 is shown in Figure 5.5. It is impossible now to discover how much was original design and how much was the result of later ad-hoc additions. It is known, however, that the curved top section, which was the only part of the beach which penetrated the air/water surface, was a comparatively recent addition. It seems likely that this was the only part of the beach which had any significant effect. The centre 1/3 of the beach was removable so that models could be brought out from the dock, and it was been common practice to replace only the top part of this section.

Figure 5.6 shows reflection coefficients measured on this beach over a range of regular waveheights and periods and also in random waves. At short periods, where the beach was long compared with the wavelength, reflection coefficients varied from around 5 per cent for large waves to about 15 per cent for small waves which surged rather than broke. At low frequencies, where the beach was short compared with the wavelength, reflection coefficients rose to around 60 per cent for small waves. The results were not entirely conclusive, but this was attributed to the difficulty of actually making the measurements. The beach did not meet the criteria which were explained in Section 5.2, in particular it was too short and steep. It is now being replaced.

5.5 Active Beaches

It has been suggested that the "absorbing" wavemaker is also - potentially - an active beach, and that if waves are generated by a machine at one end of a ship tank, then in principle a similar machine could remove them from the other end and thereby prevent reflections. The problem is how to design the control system for such a machine, and what demand to feed it with. At present, there seems little point in persuing the design of such a machine because it would obstruct the dock area of existing ship tanks. A modified tank design with a side dock, and a carriage which could be rigged from alongside the tank would be needed.

Such extensive work is unlikely to be economic when set against the adequate performance of much simpler passive beaches, and the current climate for research in marine technology.

5.6 Resonators

It will be shown in a later section of this report that good absorption of long waves is the most important requirement of a ship tank beach, and that -if necessary - this can be achieved at the price of having poor absorption of short waves. This requirement is almost opposite to the characteristics of the beaches which have, so far, been described.

One way to obtain good performance for long waves is to design a resonant termination for the ship tank, tuned to the long waves; and then to absorb energy from the resonator. Such a design would also permit the wave absorber to be optimised for any given wave spectrum, or even to be tuned to absorb the surface wake of a ship model being run in calm water.

A series of model and full-scale tests led to a design of resonator for No 1 Ship Tank at Haslar, which is illustrated in Figure 5.7. Details of the design will be reported separately (Reference 13), so only an outline is given here. A resonant chamber was set up between the vertical end wall of the ship tank and a 25 per cent porous screen which was mounted transversely at half the tuned wavelength from the end wall. At resonance, antinodes form in a standing wave at the end wall and at the porous screen. A second porous screen, of only 15 per cent porosity, was mounted half way along the resonator, at the position of the standing wave node, to absorb energy from the oscillatory horizontal flow which occurs at that point.

In this form, the device was very highly tuned. Although the reflection coefficient was very low at resonance, it was high at closely adjacent frequencies. A third screen, placed one-third of the way along the resonator, served both to increase the bandwidth and to further reduce the reflection coefficient at resonance, resulting in the performance shown in Figure 5.8. This figure shows measurements made in a number of different random seastates for screen spacings of 1.5 metres, 2.1 metres and 4.2 metres from the end wall of the tank. The screen spacing can be adjusted, whilst maintaining the approximate $^1/_3:^1/_2:1$ distance ratio, so the minimum reflection coefficient can be placed at any required frequency.

The absorber also incorporates longitudinal porous screens. These are to absorb energy from transverse modes of the ship tank which are otherwise very lightly damped and consequently very easy to excite. The longitudinal screens also provide a convenient way of strengthening the entire structure.

6. USEFUL LENGTH OF THE SHIP TANK FOR REGULAR WAVES

Previous sections have dealt with the wavemaker; the way in which waves propagate in the tank, and how the waves can be optimised at some point in the tank by windowing the input signal to the wavemaker; and the performance of the beach.

Having quantified these effects, it is then possible to design an experiment in which a model vessel is run at a fixed speed in head or stern regular waves.

A graph is drawn with distance along the tank on the horizontal axis, and time on the vertical axis. (Figure 6.1). A decision must be made about the allowable error in waveheight at the start of the test run. Assume that this must not exceed 5 per cent. From Figure 3.5(b) we see that the waveheight reaches 0.95 of the required value when

$$t\sqrt{\frac{g}{4\Pi x}} = 0.88$$

$$\text{ie when } t^2 = \left[\frac{4\Pi}{g} \times 0.88^2\right] x$$

Zero on the horizontal axis of Figure 3.5(b) corresponds to the time of arrival calculated from the group velocity of the waves. Hence, for any wave period, the group velocity line can be drawn on the graph and then plot another curved line differing from the group velocity line by the value of t (given by the plotted, above equation at any value of x).

The test run must take place in the area above this curved line on the graph. (The example chosen in the graph is for an 0.2 m, 2.5 sec wave, which has a group velocity of 2.25 m/sec in the tank.)

The original beach reflection coefficient for this wave was about 28 per cent, so setting a maximum error of 5 per cent on the contamination of the wavetrain by reflections from the beach, corresponds to incident waves of $\frac{100}{28} \times 0.05$ of the max waveheight. From Figure 3.5(b) it can be seen that waves reach this value (17.86 per cent) when

$$t\sqrt{\frac{g}{4\Pi x}} \simeq -1.25 \text{ ie when}$$

$$t^2 \simeq \left[\frac{4\Pi}{g} \times 1.25^2\right] x$$

and t is negative.

This is only an approximation because eventually we will be fixing a time-scale for Figure 3.5(a) which ensures that Figure 3.5(b) holds at the point and time in the tank where we decide to START our test run. Figure 3.5(b) does not hold at other times and places in the tank, and the actual situation at the END of the test will be somewhere between that shown in 3.5(b) and that shown in 3.4(b).

The curve given by this equation is plotted, relative to the group velocity line, for the part of the group velocity line after reflection from the beach, where x = length of tank plus distance from beach.

Remembering that we should not work within four depths of the wavemaker because of the local disturbance, we now have a triangular

area (shaded on the Figure) in which the entire test run must take place. A run at a fixed speed will be represented by a line of fixed slope superimposed on the graph. The intercept of this line with the axes is chosen to maximise the length of the line which lies within the shaded triangle. Generally the run will either start or finish four depths from the wavemaker, but only high-speed runs will use the maximum available length, which is just over 90 m in this example. A run towards the beach at 1 m/sec is illustrated on the graph, and has a maximum length of only 54 m in a tank which is 150 m long.

The last task is to fix the time-scale for the window function of Figure 3.5(a) to optimise the waves at the start of the run. For the example, the run must start 64 m from the wavemaker, 40 sec after time zero on Figure 3.5(a). This scale is given by:

$$\sigma = \sqrt{\frac{2 \times START}{g}} = \sqrt{\frac{2 \times 64}{9.81}} = 3.61 \text{ sec.}$$

Summary

We have elected to allow the monofrequency drive signal to the wavemaker to build up slowly to its full amplitude. The time-scale for the build-up, illustrated in Figure 3.5(a) has been selected so that the waves start smoothly and quickly, without overshoot of amplitude, at the time and place where our test run starts.

The times and places where the test run starts and ends have been fixed by (a) the allowable deficit in wave amplitude at the start of the test, (b) the allowable contamination by beach reflections at the end of the test, (c) the extent of the local disturbance of the water near the wavemaker.

Other limitations on the test, such as the wavemaker performance envelope and the possibility of wavetrain disintegration were discussed earlier.

7. RANDOM WAVES

Random waves are more appropriate for testing nonlinear effects, and compared with spectral methods, the summation of the results of many regular wave tests to obtain a transfer function is tedious experimentally. Tests on both nonlinear phenomena (eg the overtopping of a sea wall) and linear phenomena therefore benefit from random wave methods, but for different reasons.

It is not the purpose of this paper to reproduce material on statistics and signal processing, which can be found in many text books, but some comments on randomness, as it affects ship tank testing, must be made.

Random signals are defined statistically by an amplitude probability density function and spectrally by a spectral energy density function. The first defines the probability of the signal (in our case the instantaneous water level) having a particular value at any instant in time. The second defines the average power per unit frequency as a function of frequency. In the context of waves in tanks, a random sea

will be defined as one with a continuous, as opposed to a line spectrum. An irregular sea will be defined as one with a large number of spectral lines, but not so many that the individual lines are indistinguishable. A typical number of spectral lines in an irregular sea might be 20.

7.1 Statistical Parameters

Wideband continuous spectrum signals generally have a gaussian amplitude probability density function, which can be characterised by a mean value and a standard deviation. Band limited signals deviate from the gaussian pdf, often having a long 'tail' to the pdf indicating the remote probability of very large signal amplitudes. Waves are usually measured by electronic means, and an electronics engineer would generally measure the resulting signal by defining its root-mean-square (rms) value over some time interval. The time interval would be chosen, taking account of the bandwidth of the signal, so that measurements made at different times, but over the same interval, would have the same rms value. If this is possible, the signal is said to have stationary statistical properties. Civil and naval architects often measure waves using a parameter which they call the significant waveheight. This is based on a subjective assessment of the sea, and it is statistically equivalent to the mean height of the highest one-third of the waves. For a gaussian signal, it is usually computed by taking four times the rms waveheight. (For this reason it is important not to use random wave analysis programs to analyse regular wave tests - the peak to peak height of a sinewave is not four times its rms value!)

7.2 Spectral Parameters

The spectrum of a random sea is defined by the mean-square amplitude per unit of frequency (units: m^2 -sec or m^2/Hz) as a function of frequency. Various studies have led to "standard" spectra being used for particular types of test. The standard spectra are specified by equations with one or two variable parameters which depend on physical factors affecting the sea which is being modelled (such as windspeed). Examples are JONSWAP (Joint North-Sea Wave Project) and Bretschneider (the ITTC open ocean standard spectrum). The equations define the relationship between the spectral energy density and frequency for a continuous spectrum, but any practical laboratory experiment - because of its finite duration - will effectively be excited by a line spectrum, albeit one with very many lines. In this case, the amplitude of each spectral line must be adjusted to achieve the spectral envelope which has been defined. It is helpful if the form of the equation is such that the zero, second, and fourth moments are analytic, because this assists the prediction of the statistical parameters of the sea.

Example

The Bretschneider spectrum is defined by the equations

$$s(f) = 0.313 \left[\frac{fp^4}{f^5}\right] H_s^2 \exp -1.25 \left[\frac{fp}{f}\right]^4$$

where H_s is the significant waveheight in metres

and f_p is the modal frequency in Hertz

This function is plotted for a significant waveheight of 1 m and a modal frequency of 1/10 Hz in Figure 7.1. The area under this curve is 6.26×10^{-2} m², the rms signal level is therefore $\sqrt{6.26 \times 10^{-2}} = 0.25$ m, one quarter of the significant waveheight which was specified.

7.3 Real Seas

The fact that measured seas are characterised in spectral and statistical terms has led naturally to the methods by which they are modelled in ship tanks. However it is important to realise that, although we describe a sea in a way which assumes that it is the summation of a large (possibly infinite) number of sinusoidal components of random relative phase, this is not necessarily the way in which nature generates real seas.

Real seas are generated by an exchange of energy at the water surface between wind and waves. This exchange must take place over a considerable time (the duration) and distance (the fetch) before the sea becomes fully developed. A fully developed sea is one which will not change if the duration and fetch are extended. Prior to reaching this condition the sea builds up through a continuous process of change from completely calm. Initially, small, short capilliary waves form on the calm surface. These increase in amplitude until they are large enough for non-linear effects to gradually transfer energy from the short waves into slightly longer ones. As the process continues longer and longer waves, of larger and larger amplitudes appear in the spectrum until a stage is reached when the energy input from the wind is in equilibrium with the energy lost by dissipation. This process is just like the Benjamin-Feir disintegration of regular waves in ship tanks which was described earlier, and in the reference it is suggested that a real sea should be considered as a single amplitude-modulated non-linear wave rather than the sum of many sinewaves. Subjectively, wave records from real seas look more like a modulated carrier than a completely random signal, a fact which shows in the spectrum as a well-defined, and fairly narrow, peak.

Very high wind speeds do not often occur over long fetches or for long durations, so fully developed seas are rare. For this reason, particularly near coasts, winds of say Force 6 blowing for a long period may build up bigger seas than gale force winds over a short period. Other factors affect seas near coasts, particularly reflection, funnelling, the steepening and breaking of waves as they move into shallow water, and the very rapid steepening and breaking of waves which run into opposing currents.

8. PROPAGATION OF RANDOM WAVES

Because this paper is intended to be descriptive rather than mathematical, most of this section is written assuming that the random sea consists of the summation of a large number of "Airy" sinusoidal components, and that each component behaves exactly as it would behave in the absence of the others. This is obviously a very simplified

view of the truth, but it yields useful results which would be obscured by attempts to include the bound harmonics of each wave frequency, and the higher-order interactions which are really present. The only exception is in the consideration of the performance of the beach, where the wave breaking criteria discussed earlier cannot be applied to each individual frequency component because wave breaking is a very non-linear process.

Therefore it is assumed that everything covered in Sections 2 and 3 about regular waves is also true of random or irregular waves. In particular:

a. Each component travels with a celerity given by

$$C^2 = \frac{g\lambda}{2\pi} \tanh \left[\frac{2\pi D}{\lambda}\right]$$

b. Each component has a group velocity given by

$$V = C \left[\frac{1}{2} + \frac{\frac{2\pi D}{\lambda}}{\sinh \frac{4\pi D}{\lambda}}\right]$$

c. Waves will break when the summation of all the components results in a wave with a peak which has an included angle of less than 120 degrees.

It can be anticipated that breaking waves might occur anywhere, but not everywhere, in the tank because of the random phasing of individual components, and that effects such as disintegration should be undetectable because the amplitude of each sinewave component will be small (the actual amplitude of each depending on how many components are present in all).

In Reference 9 it is shown that the maximum value of a random variable can be predicted from its energy density spectrum S(f), so that the maximum crest height in the ship tank can be predicted if the spectrum (to model scale) is known. Conversely, it is possible to calculate the maximum rms signal level which can be contained within the wall height of the tank. It will be shown later that the signal generator which drives the wavemaker must impose a further limitation on the ratio of crest: rms waveheights. For a given spectrum, this ratio (called the crest factor) can be set during the design of the signal generator. Once the signal generator is designed, the crest factor will vary slightly between spectra. Typical values are about 4-5.

8.1 Beaches

The original beach reflection coefficients which were measured for regular waves are of no use in predicting quantitatively how the beach will perform in irregular or random waves, but they provide the qualitative idea that the beach would probably reflect long waves (low frequencies) rather well.

It was therefore essential to re-evaluate the beach using random incident waves. This is obviously more difficult than it was with

regular waves. More wave probes (2 or perhaps 3) were needed, and measurements were only possible over a limited bandwidth without re-siting the probes. Reference 10 is an example of the methods employed. Figures 5.6 and 5.8 include random wave results from both the original beach and the new resonant abosrber of No 1 Ship Tank.

Civil engineers are used to making such measurements on model and full size beaches and breakwaters, but it is unusual to see a ship tank beach tested in random waves. Random wave tests usually indicate values of reflection coefficient comparable with those measured using very small regular waves, than regular and the dependence on incident amplitude is not as strong. Presumably this is because reflection is a non-linear process which happens in the time domain (each wave being composed of energy from many spectral components and the reflection depending on whether or not the wave breaks on the beach) whereas the results are expressed as mean values in the frequency domain.

It is possible that Benjamin and Feir's ideas about a different model for wind waves are more appropriate when handling this sort of problem. However, our current methods of generating waves are based on the linear superposition of sinusoidal components, and it is necessary to assume the same model when characterising the beach.

9. USEFUL LENGTH OF THE SHIP TANK FOR RANDOM WAVES

Section 6 described a graphical method for optimising a test run in regular waves. On the assumption that the random sea is a linear superposition of regular components, this method can be extended to random seas. Taking as an example, the Bretschneider spectrum of Figure 7.1, to a model scale of 1/25th, the time-scale and the velocity scale will be 1/5. The lowest frequency which will be present in the model spectrum will be 0.25 Hz (0.05 x 5) and the highest frequency will be 1.33 Hz. (For reasons which will be explained in the next section, the highest model frequency will be $\frac{16}{3}$ times the lowest frequency for this spectrum.)

As with regular waves, we can plot our "allowable triangle" diagrams for the highest and lowest frequencies separately. We then superimpose them to produce Figure 9.1, in which we have ensured the maximum overlap of the two triangles by shifting the time axis of one relative to the other.

The random sea can be made to meet the specification (ie less than 5 per cent error on the amplitudes) only in the area which is common to both triangles, only if the gaussian window is applied to each frequency component as it is introduced into the spectrum, and only if a successive time delay is also imposed as progressively lower frequency components are added to the spectrum. The lowest frequency component must be introduced about 80 seconds after the highest component in this example spectrum.

At a model speed of 1 m/sec, only 30 m out of the 150 m total length of the tank can be used if the sea is to be within 5 per cent of specification.

Some comments must be made about this apparently appalling result.

a. Most model tests are comparative rather than absolute, so greater errors can probably be tolerated if steps are taken to ensure that the position/time histories of all model runs are the same. However, it is not uncommon to see the results of a model test on a proposed new design compared with prototype data from an existing design. This could be very misleading.

b. The result has been plotted using data on the original beach of No 1 Ship Tank. It is left to the reader to examine the very substantial improvement afforded by using the new resonator.

10. A NEW SIGNAL GENERATOR

Some comments on the design of wavemaking machines were made earlier in Section 4. In this section, it is assumed that the wavemaker is a linear device with a transfer function between input voltage and generated waveheight like the one measured on the Haslar tank, and shown in Figure 4.3. This is a considerable simplication of the truth, and - in fact - ignores some effects which are of very great importance in some types of test. However, discussion of these effects is outside the scope of this paper. Some concession will be made to the real situation by allowing for the possibility that the voltage/waveheight transfer function may vary slightly from one wave spectrum to another.

Given this transfer function and the required wave spectrum, one can easily calculate the spectrum of input voltage which must be fed to the wavemaker. Initially, this spectrum must be time-dependent to provide the necessary delayed introduction of low frequencies at the wavemaker. Having applied this signal to the wavemaker, and measured the spectrum of the resulting waves, it may be necessary to adjust the transfer function slightly and repeat the process in order to improve the accuracy of the wave spectrum.

There are several possible methods of producing a suitable input signal. Hardware for each of the methods is described in References 11 and 12, although current practice is to emulate the hardware with computer software. The methods fall into 3 groups:

a. Analogue noise source plus analogue or digital filters.

b. Sum of sinewaves.

c. Digital noise source plus digital filter.

a. Analogue Noise Source and Filters

This technique has serious disadvantages for this application. Most analogue noise sources (eg zener diode) exhibit long-term variations in rms output. It is also impossible to exactly repeat a particular time-history of signal (unless the signal is tape-recorded), and such repeats are valuable when comparative tests are being made on different designs of vessel. The use of analogue filter banks causes difficulty because phase shifts

prevent the signals from individual filters adding arithmetically, and a spiky spectrum results. Attempting to design special filters requires an attempt to describe the signal spectrum in terms of the poles and zeros, of the equivalent filter which is difficult, and requires different filters for each spectrum. The method was common 2 decades ago, but is not used now.

b. Sum of Sinewaves

Early mechanical devices to implement this method were based on the designs of the mechanical computers which were once used to produce tide tables from the periodic motion of the moon, sun, and planets relative to the earth. It was difficult to repeat time-histories because small errors in setting the initial phases of the sinusoidal components resulted in signals which diverged increasingly with time. It was only possible to produce irregular signals with a limited number of spectral lines; random or pseudo-random signals were impossible.

Today, sum of sinewaves techniques can be implemented on a computer. Time histories can be repeated, and the number of lines in the spectrum is limited only by the amount of time which is available for the computer to calculate the signal. The method also lends itself to the delayed introduction of lower frequencies, although applying a variable time-scale gaussian window to the start of each frequency component is slightly difficult. One disadvantage is that it is not a real-time method, especially if a continuous or near-continuous spectrum is required. This makes the iterative process, of generating waves and adjusting the transfer function to improve the accuracy of the spectrum, very tedious indeed. A second disadvantage is that the natural statistics of wave grouping are not reproduced by a signal consisting of a relatively small number of superimposed sinusoids.

c. Digital Noise Source and Variable Digital Filter

This method, which uses a pseudo-random binary sequence (PRBS) generator as noise source and a non-recursive variable digital filter to shape the spectrum, was originally implemented in hardware and called a wave spectrum synthesizer (12). It is now implemented in software on micro or mini computers, but the principle is unchanged. Calculation of the necessary filter weights involves taking a Fourier transform of the required spectrum, but thereafter, even a small microcomputer can generate near-continuous spectra in real time. The method also has the advantage that control of the signal repeat time, and hence the number of lines in the spectrum, can be obtained independently of the shape of the spectrum. This means that the process of iteration to obtain an accurate spectrum can be done speedily using a spectrum with a limited number of lines, and then the number of lines can be increased, without changing the spectral envelope, ready for a model test run.

Generally, linear phenomena are tested using few lines, and the results presented spectrally whereas non-linear phenomena are tested with many lines in the spectrum and the results are presented statistically. Because the filtered (band limited) PRBS has gaussian statistics, the method produces seas which are both spectrally and statistically correct, and any given time history can be regenerated exactly.

This technique is in almost universal use in civil engineering hydraulics, for both long and short-crested random and pseudo-random seas, but for ship tank use, a modification is required to enable the progressive introduction of low frequencies at the start of the test. The modification requires the addition of a time-varying digital filter between the non-recursive filter which shapes the spectrum, and the digital to analogue converter, as shown in Figure 10.1.

The characteristic which this filter must have in the frequency domain is shown in Figure 10.2, for an example, corresponding to the Bretschneider spectrum of Figure 7.1, modelled to a scale of 1/25. At any frequency, the gain will vary from 0 to 1 at a time given by the vertical axis of the triangle diagram of Figure , and over a time interval corresponding to Figure 3.5(a). Therefore, both the frequency response and the slope of $\left[\frac{\text{cutoff frequency}}{\text{time}}\right]$ for the filter must be variable, depending on position and time at which the model test run will start.

Regular Waves

The spectrum synthesizer, although developed for the generation of pseudo-random waves, is also suitable for regular waves, and the time-varying filter which has been described is suitable for both.

In order to generate regular waves, the shift register weightings for the non-recursive filter are changed to correspond to equally spaced ordinates on a sinewave. The exclusive-OR gate is disconnected, and a direct connection made from the output of the last stage of the shift register back to the input of the first. A single "1" is preset somewhere in the shift register and recirculated. One cycle of the output sinewave is produced each time the "1" traverses the length of the register, so the sinewave frequency is directly derived from the shift register clock frequency. The time-varying filter serves to introduce the sinewave slowly, meeting the criteria layed down earlier for optimising the generation of regular waves.

Experiment Design

Because the spectrum synthesizer is implemented on a small computer, the same machine can be programmed to design the complete experiment, by - in effect - repeating the calculations which were used to produce Figures 6.1 and 9.1 in this report. the computer can then both generate the drive signal for the wavemaker and also issue instructions as to when and where the ship tank carriage motion should start and end, and also when to start and stop acquiring measurements from the model under test.

In the case of the new resonant wave absorber, the computer can also be programmed to issue instructions as to the optimum positioning of the porous screens, so that the length and accuracy of each test run can be maximised.

11. SUMMARY

This report has discussed in qualitative, and sometimes rather simplified terms, the main difficulties encountered when modelling regular and random long-crested waves in ship tanks.

A method for designing an experiment, so that the waves which a model ship encounters have minimum errors in amplitude, has been developed.

It has been shown that the performance of the beach in a ship tank is of primary importance, and that longer beaches are advantageous if they absorb long waves more effectively.

A modification to the equipment employed by civil engineers to test stationary structures in waves has been described. The modification enables models in translation to be tested according to the experiment design mentioned above.

12. ACKNOWLEDGEMENTS

The spectrum synthesizer was originally developed by a team consisting of the author, Mr G Gilbert, and Mr M J Wilkie at the Hydraulics Research Station, Wallingford, Oxon.

The modifications to it, described in the report, have resulted from discussions between the author and Geoff Gilbert, and a design study which ARE(Haslar) commissioned Hydraulics Research Ltd (now privatised) to undertake. The contribution of Geoff Gilbert to this work is gratefully acknowledged by the author.

Mr J Mitchell, of the Civil Engineering Department at Portsmouth Polytechnic is thanked for urging the author to persevere with the contents of Appendix 1, and for his efforts in examining the potential of resonant wave absorbers.

REFERENCES

1. Airy G B. On Waves and Tides. Encyclopeadia Metropolitana. Vol 5. Page 289 (1845).

2. Stokes G G. Proc Cambridge Philosophical Society. Vol 3 Page 441 (1847).

3. Gilbert G, Thompson D, Brewer A. Design Curves for Regular and Random Wave Generators. J Hydraulic Research. Vol 9 No 2 p 163 (1971).

4. Gilbert G. Wavemaker Signal for a Ship Tank. Hydraulics Research Report No. EX1472. H R Ltd Wallingford Oxon. (1986).

5. Michell, J H. On the Highest Waves in Water. Phil Mag (5) 36, page 430-435. (1893).

6. Benjamin T and Feir J. The Disintegration of Wavetrains on Deep Water. J Fluid Mechanics Vol 27. Page 417. (1967).

7. Iversen H W. Laboratory Study of Breakers, Gravity Waves. Nat Bureau of Standards (US). Circular 521, (1952).

8. Saville, T. Wave Run-up on Shore Structures. Transactions ASCE Vol 123 Page 139-150. (1958).

9. Cartwright D E and Longuet-Higgins M S. The Statistical Distribution of Maxima of a Random Function. Proceedings of Royal Society A, 237 Page 212. (1956).

10. Mansard E and Funke E. The Measurement of Incident and Reflected Spectra using a Least Squared Method. Proceedings of 17th International Conf. on Coastal Engineering, Sydney Australia. March 1980.

11. Fryer D K and Wilkie M J. The Simulation in the Laboratory of Random Seas and their Effects. IERE Conf. on Instrumentation in Oceanography Bangor, North Wales, September 1975.

12. Fryer D K, Gilbert G, Wilkie M J. A Wave Spectrum Synthesizer. Journal of Hydraulic Research, 11, No 3. Page 193. (1973).

13. Fryer D K. Waves in Ship Tanks Part 3 : A Resonant Wave Absorber. AERETM(UHU)89306, ARE Haslar, (July 1989).

SYMBOLS

c speed of sound.

g acceleration due to gravity (m/sec^2).

h wave amplitude (peak).

m mass (kg).

x linear distance along ship tank (from the wavemaker) (m).

z distance below surface (m).

C Celerity (phase speed).

D depth (m).

E modulus of elasticity (N/m^2).

F_n Froude number.

H waveheight (peak to peak).

L linear distance

M Mach number.

R_n Reynolds number.

S Wavemaker stroke (peak to peak).

T Wave period (sec).

V velocity.

W_n Weber number.

ξ horizontal displacement from mean position.

λ wavelength.

μ viscosity ($N\text{-}sec/m^2$).

η vertical displacement from mean position.

ρ density (Kg/m^3).

σ surface tension (N/m).
standard deviation.

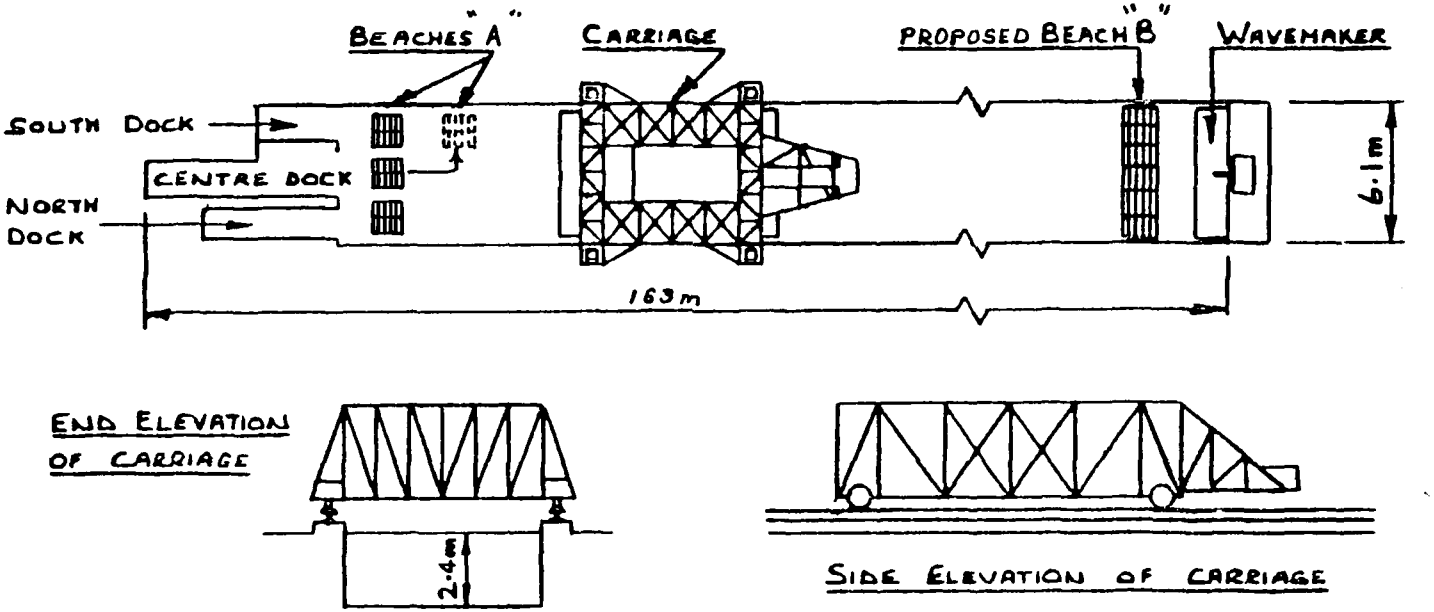

FIG. 1-1. No. 1 SHIP TANK AT A.R.E. HASLAR

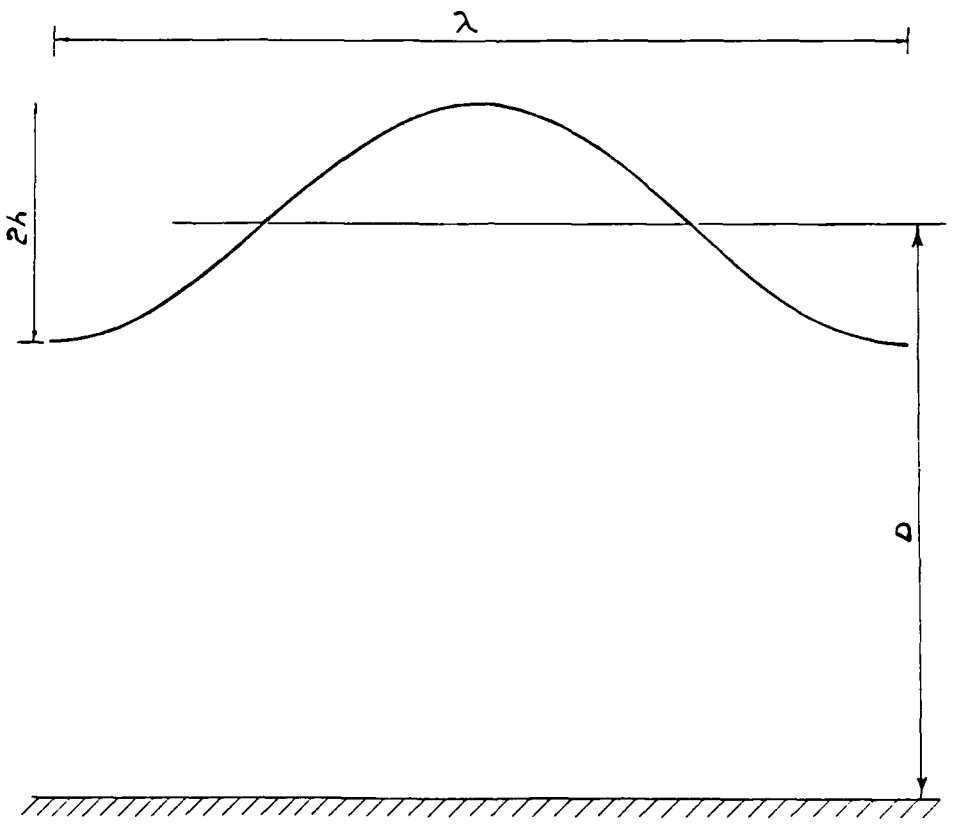

FIG. 2·1. SURFACE FORM OF REGULAR WAVE (AIRY)

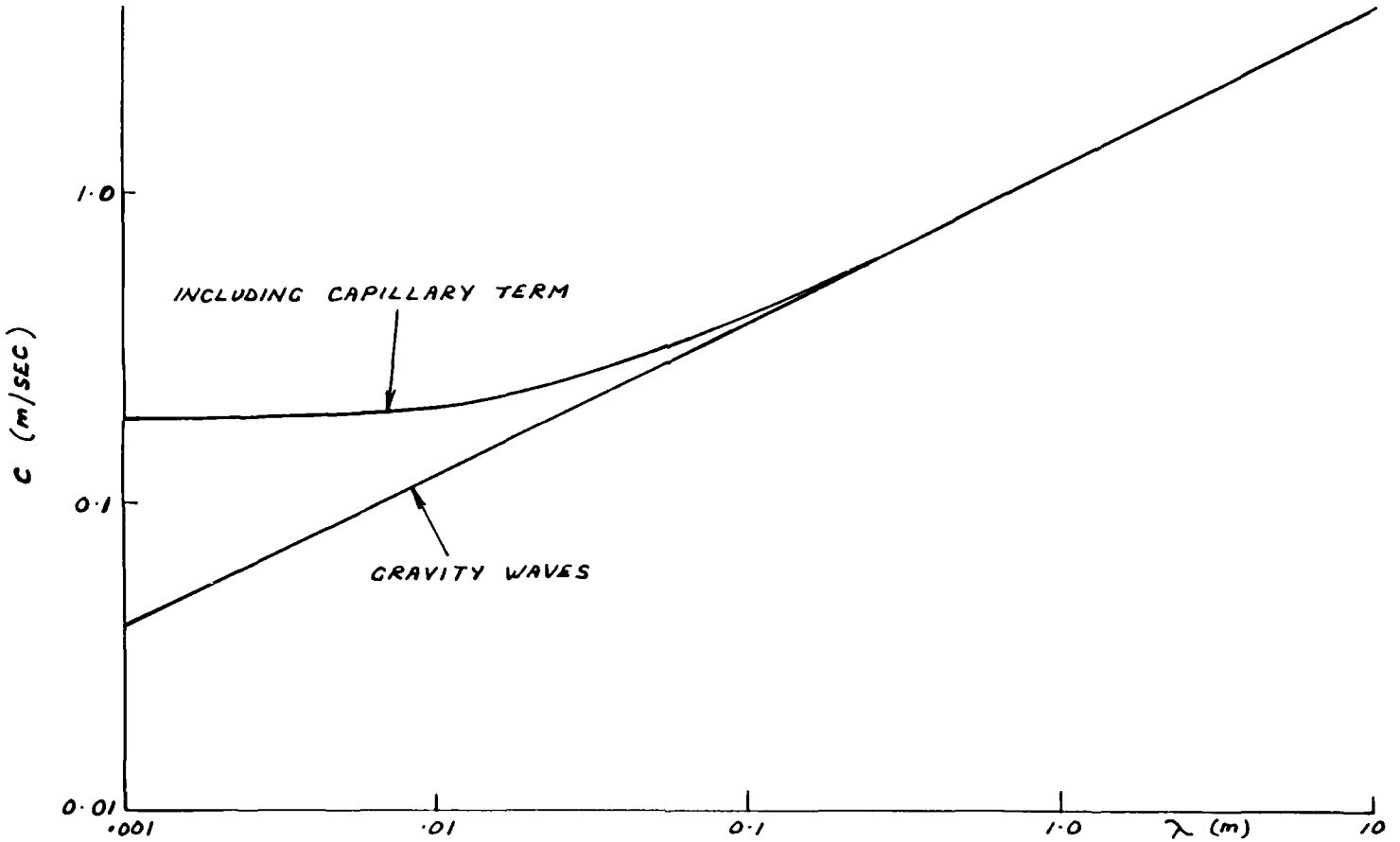

FIG. 2·2. GRAPH OF CELERITY VS WAVELENGTH

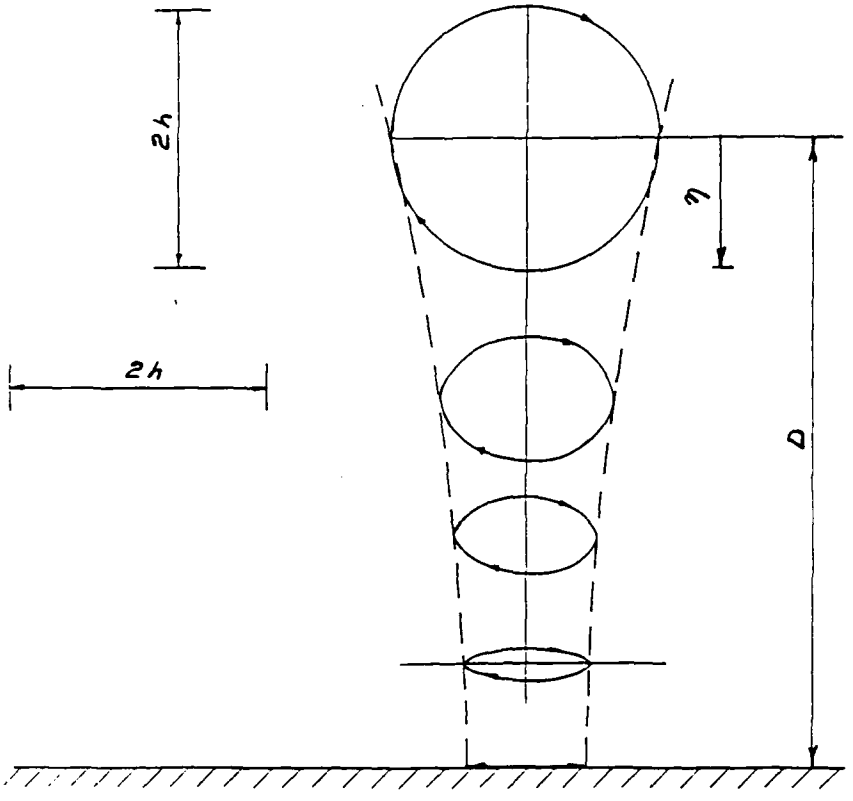

FIG. 2·3. PARTICLE ORBITS (AIRY) H = 1m λ = 10 m

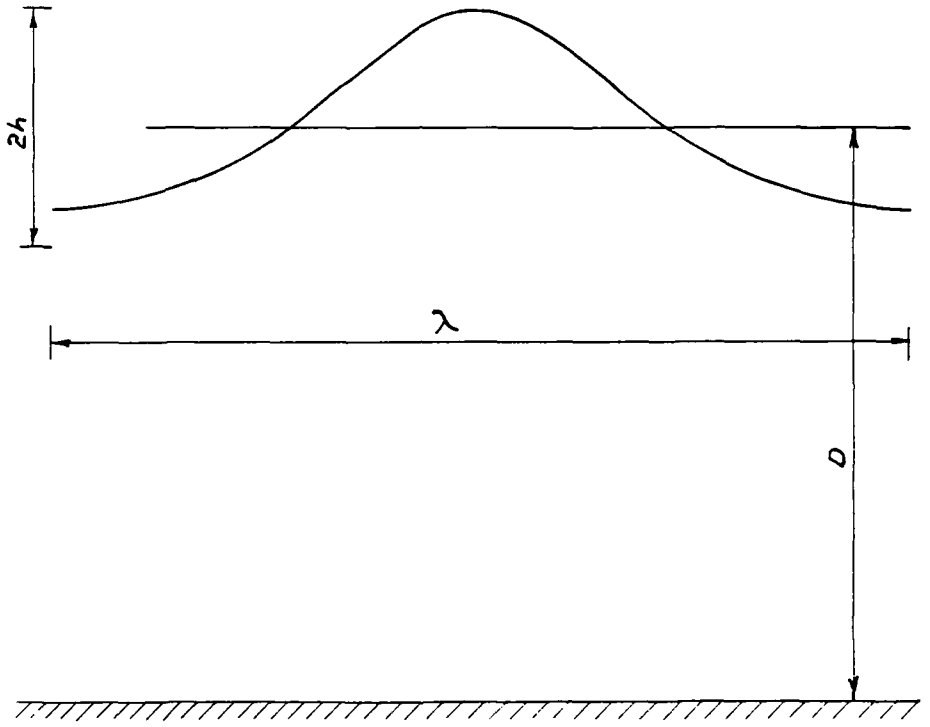

FIG. 2·4. SURFACE FORM OF REGULAR WAVE (STOKES)

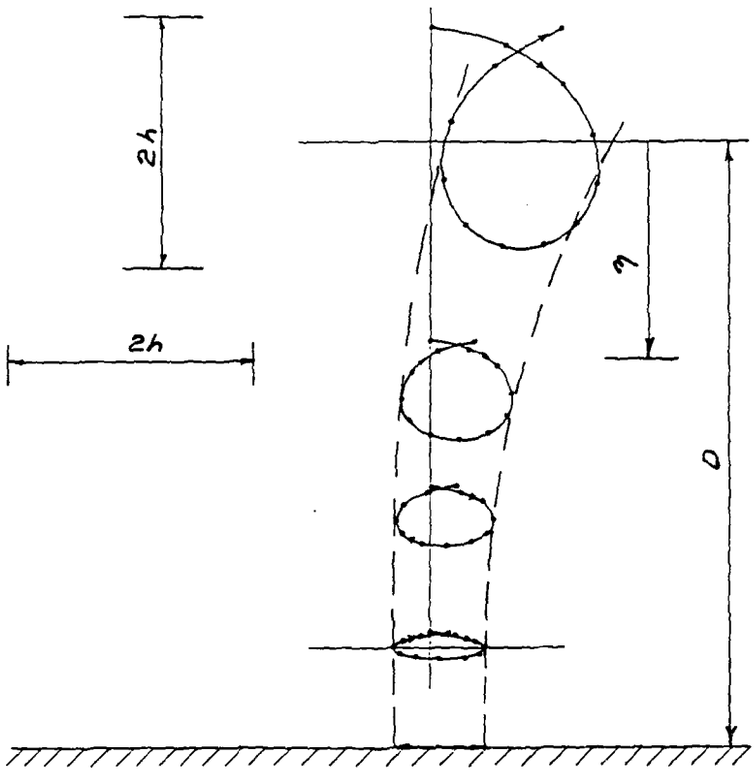

FIG. 2.5. PARTICLE ORBITS (STOKES) H = 1m λ = 10m

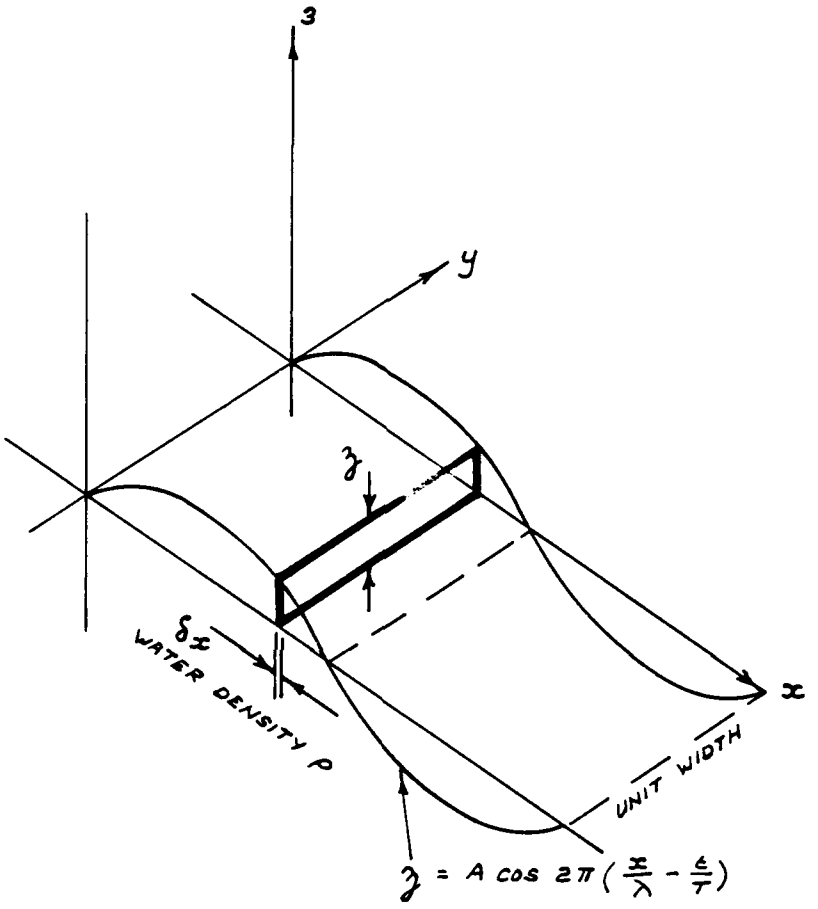

FIG. 3·1. POTENTIAL ENERGY PER UNIT SURFACE AREA

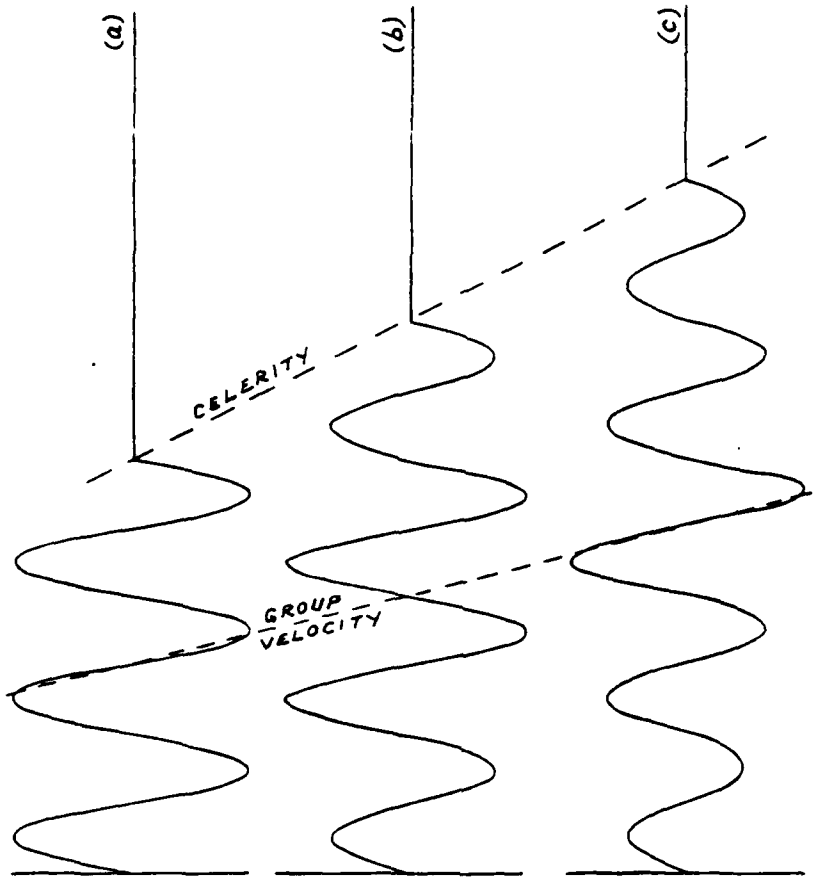

FIG. 3·2. PROPAGATION OF A WAVE GROUP

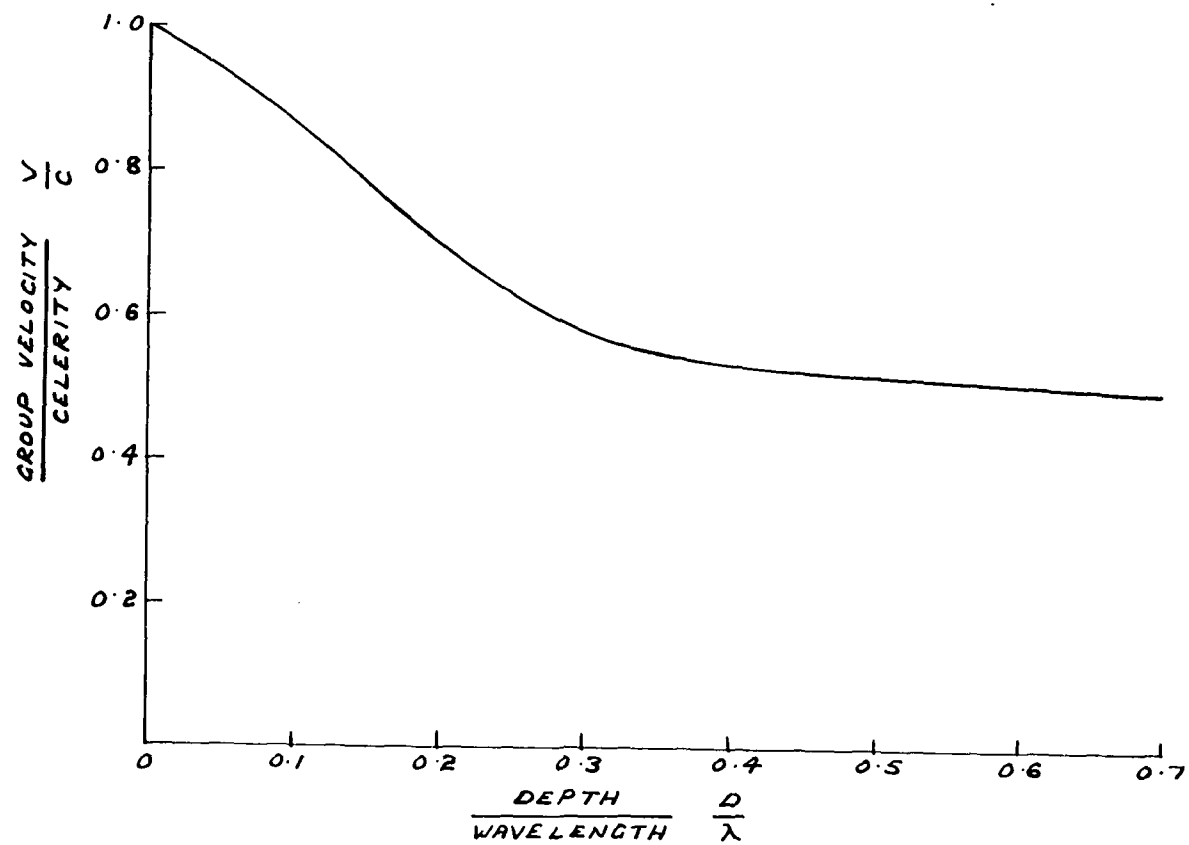

FIG. 3.3. VARIATION OF GROUP VELOCITY AND CELERITY WITH DEPTH AND WAVELENGTH

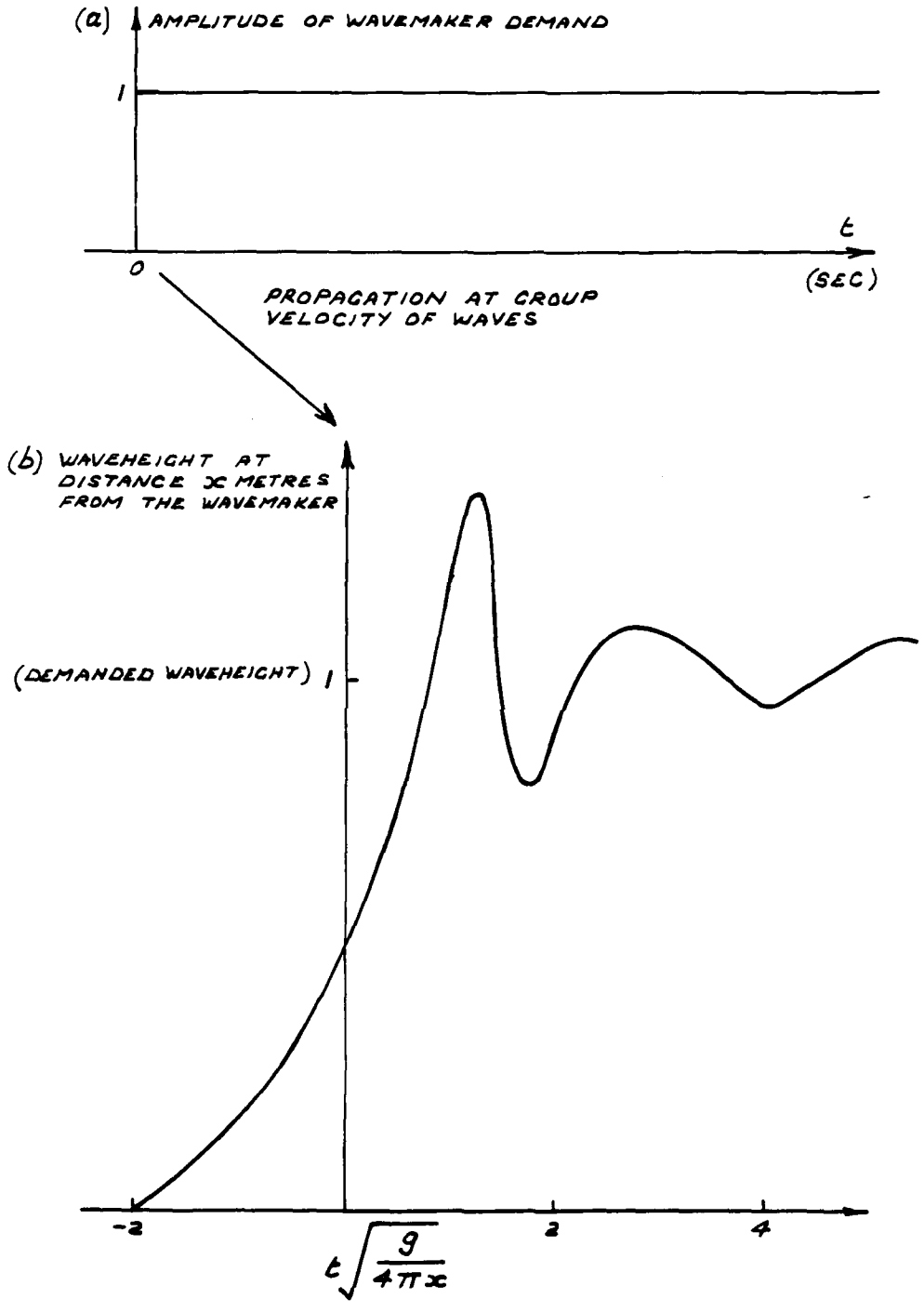

FIG. 3·4. HISTORY OF WAVE AMPLITUDES—INSTANTANEOUS START

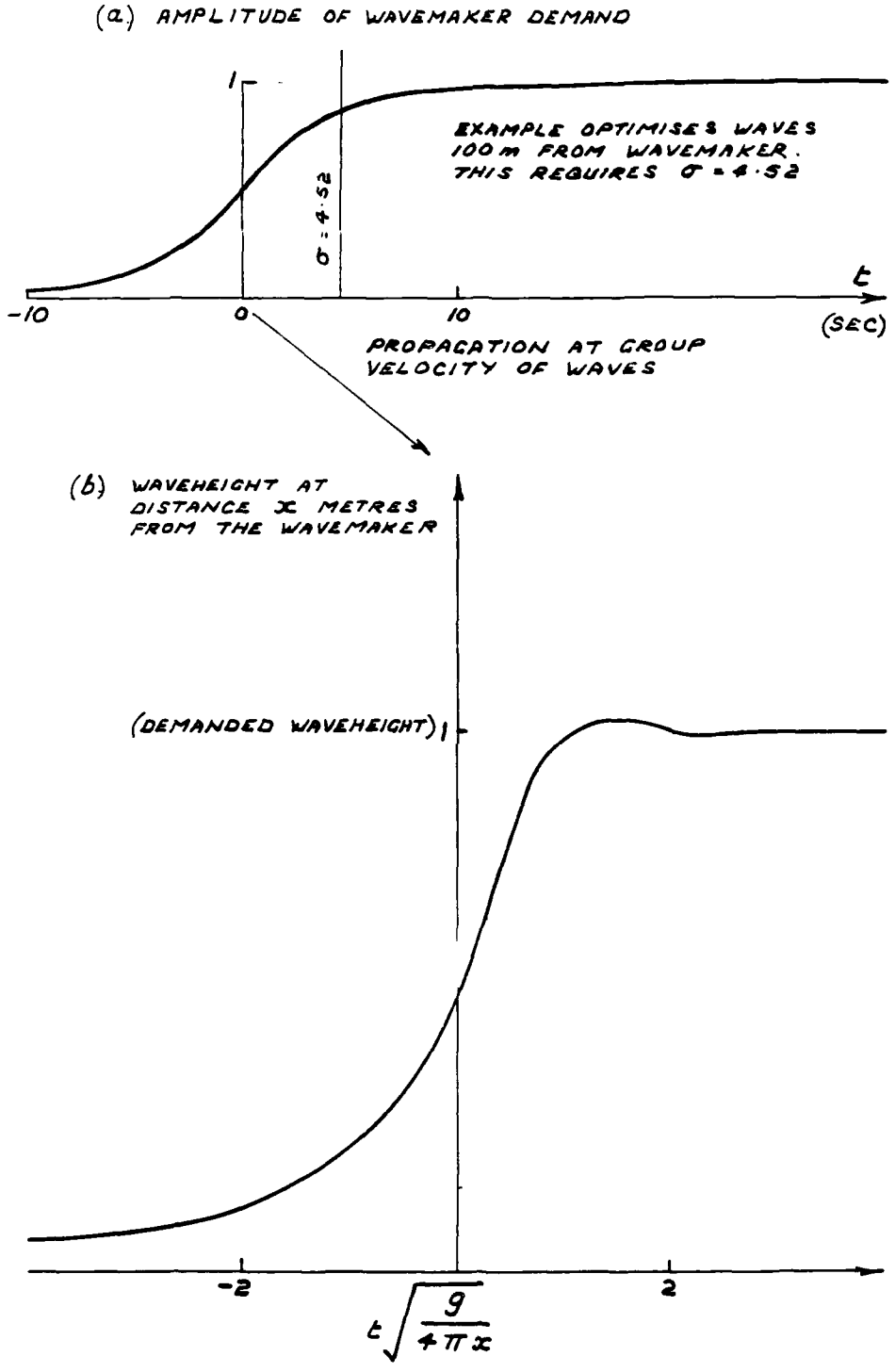

FIG 3·5 HISTORY OF WAVE AMPLITUDES - SLOW START

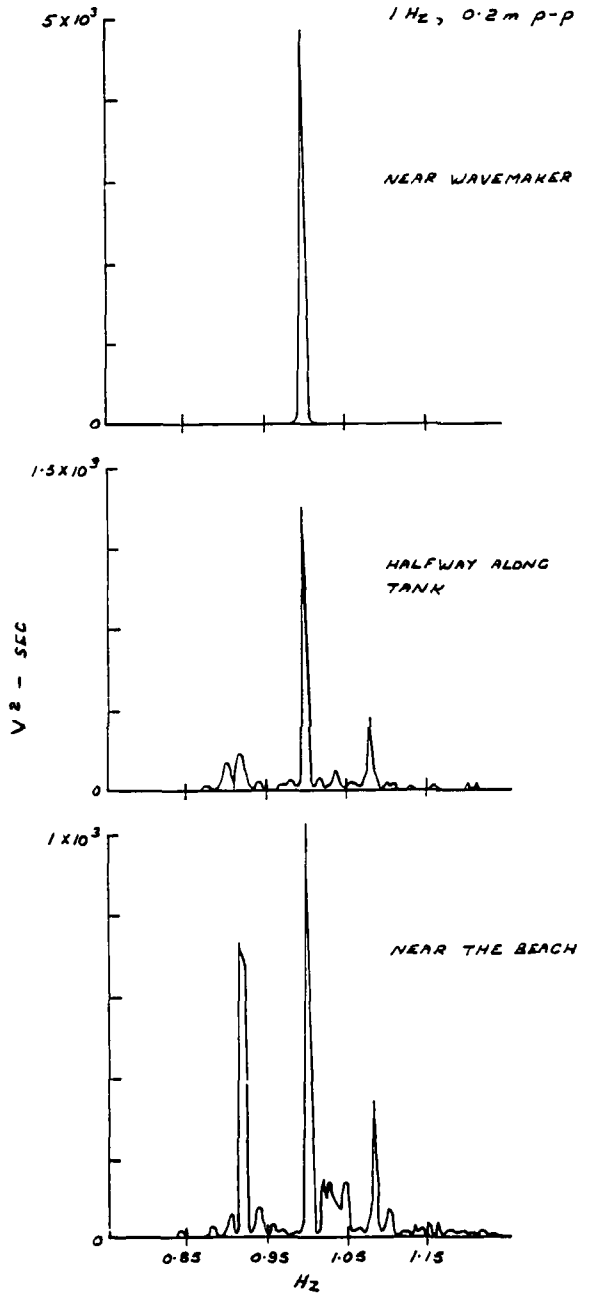

FIG. 3·6. DISINTEGRATION OF REGULAR WAVES

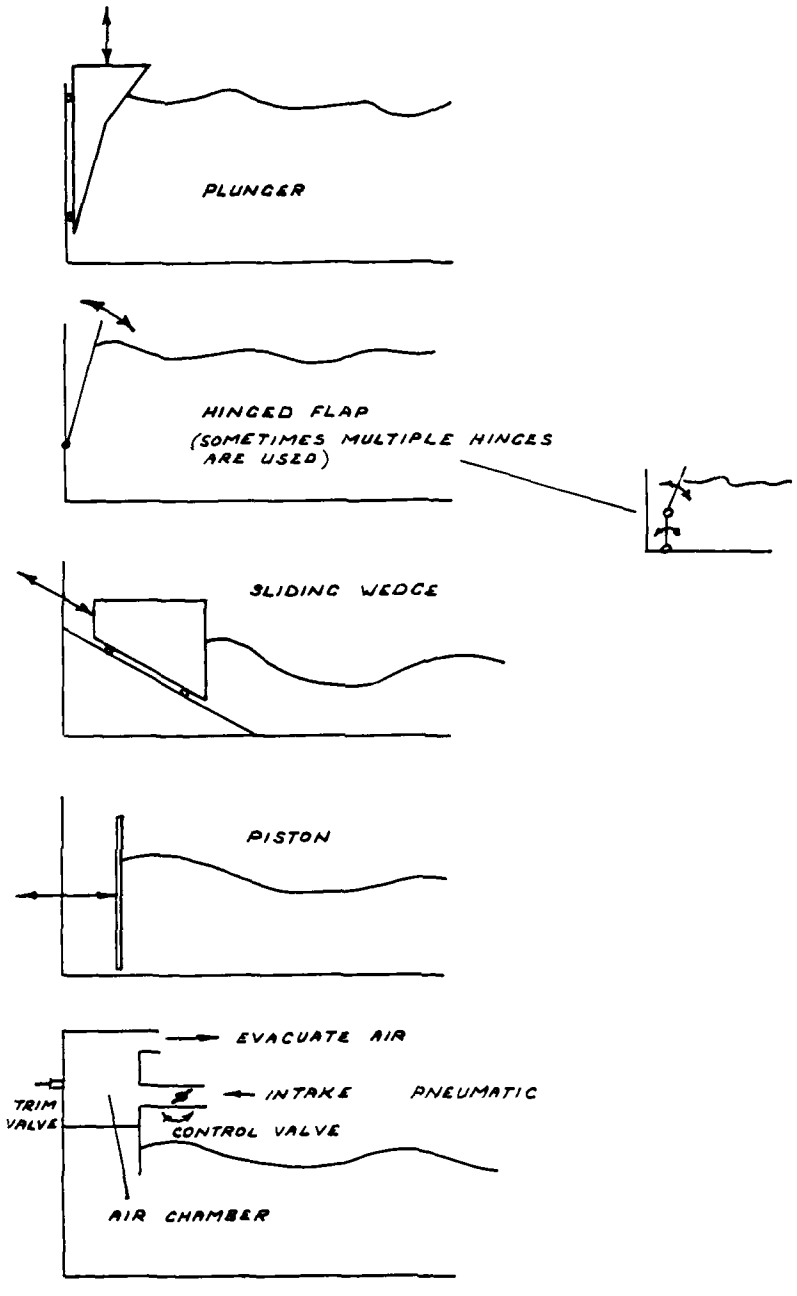

FIG. 4.1. TYPES OF WAVEMAKER

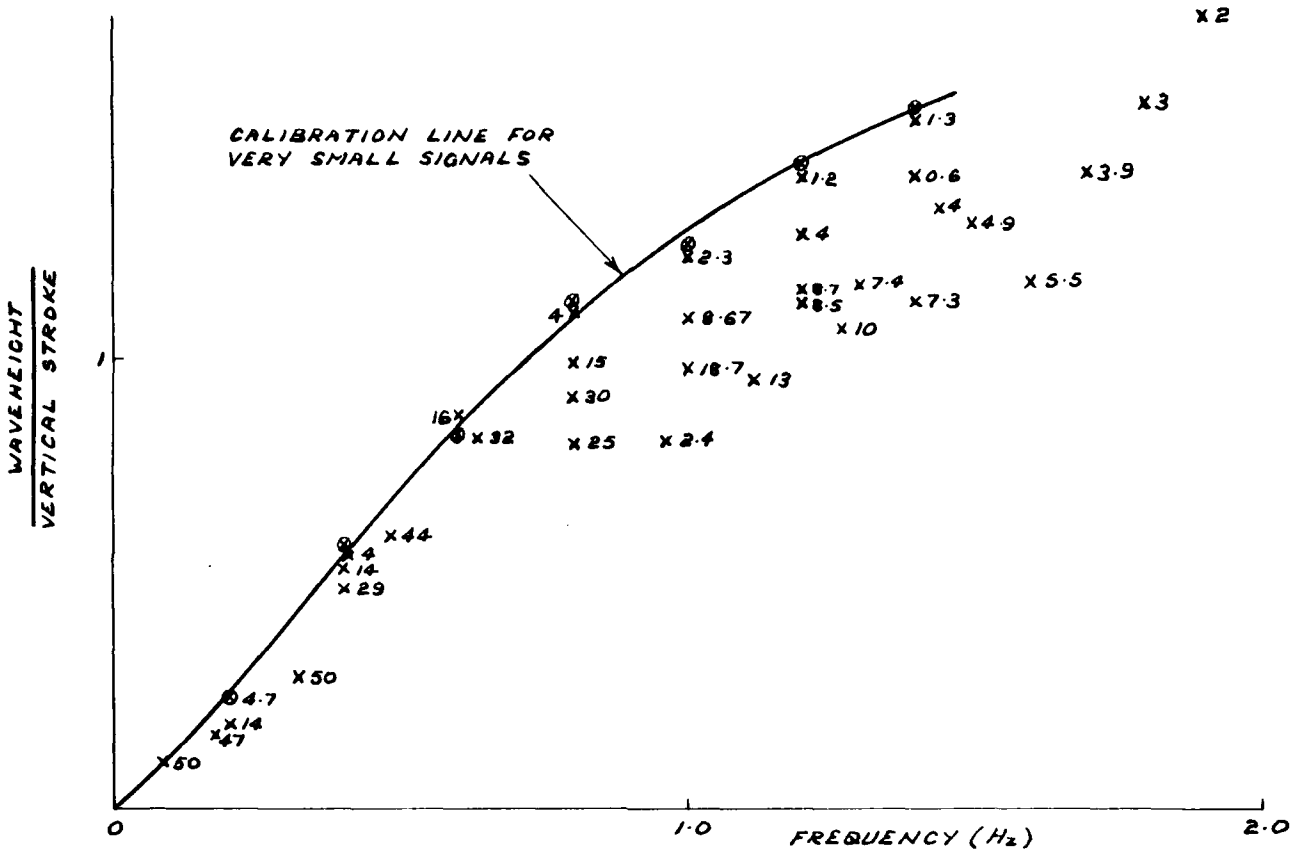

FIG. 4·2. No. 1 SHIP TANK WAVEMAKER CALIBRATION

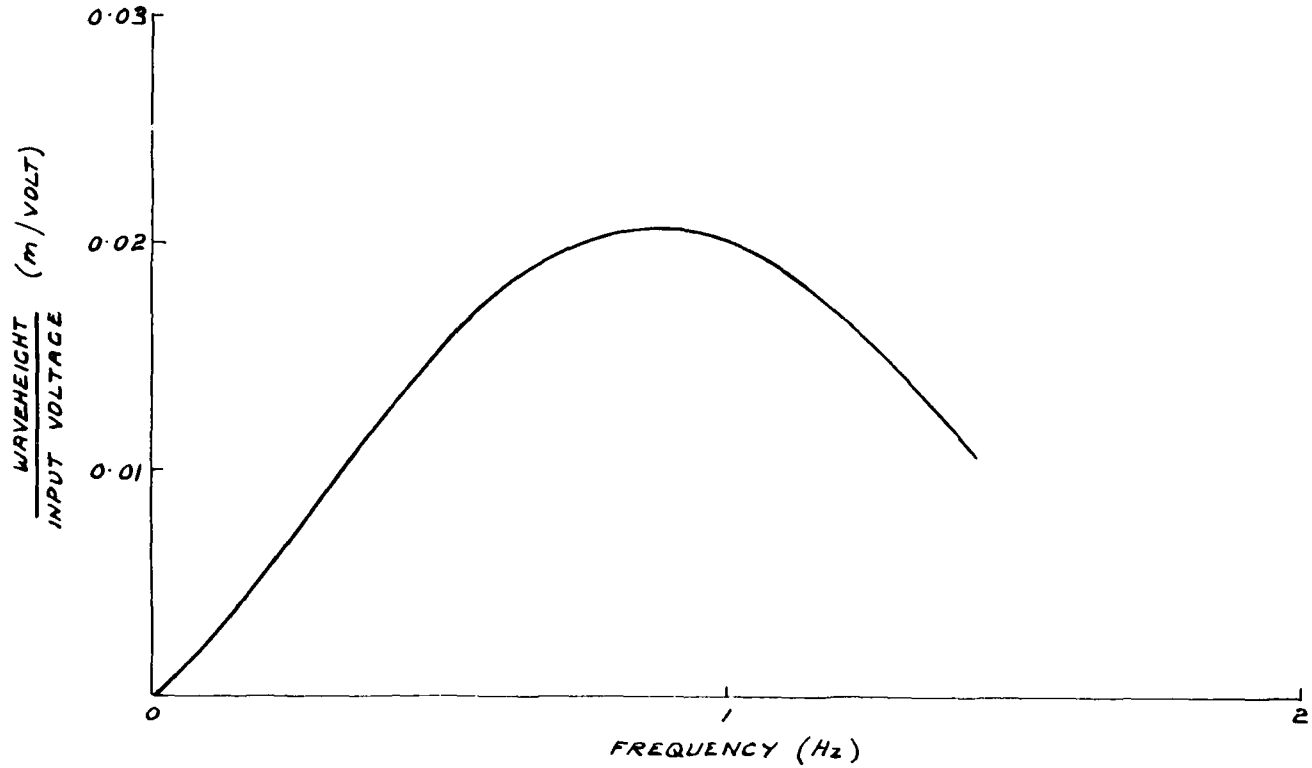

FIG. 4·3. No 1 SHIP TANK WAVEMAKER CALIBRATION

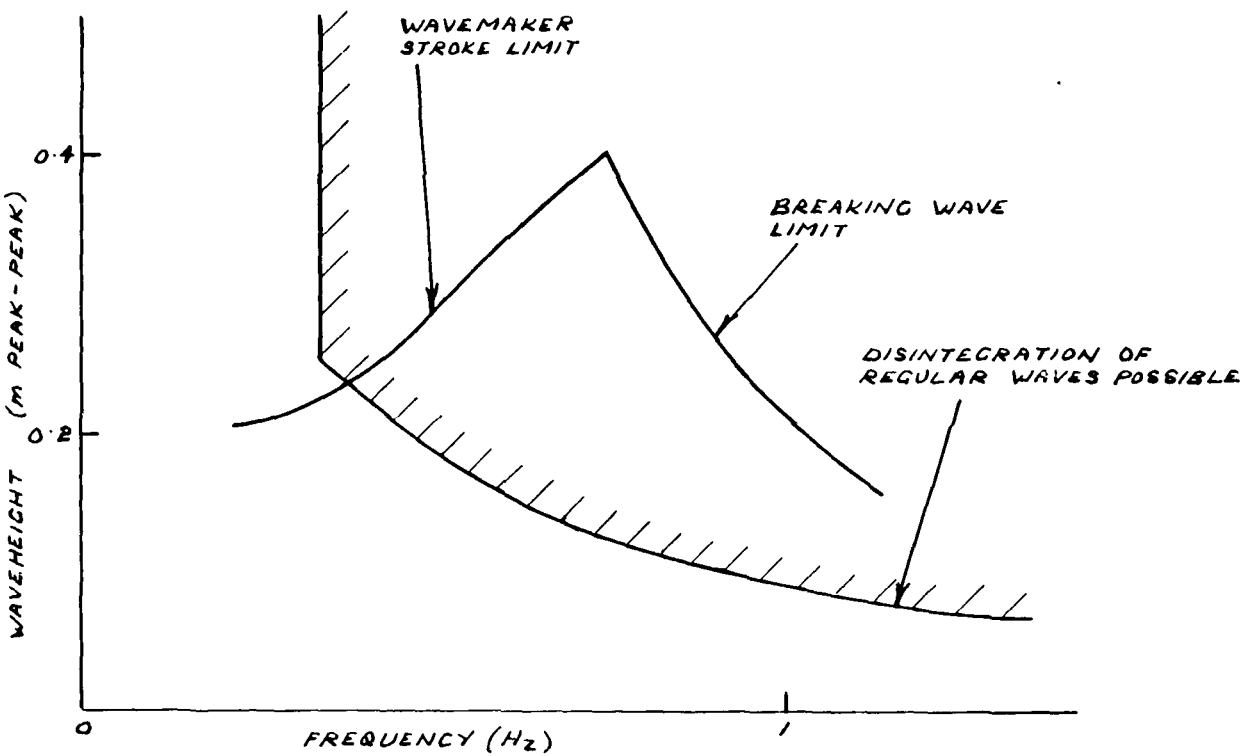

FIG. 4 · 4. No 1 SHIP TANK – PREDICTED PERFORMANCE LIMITS

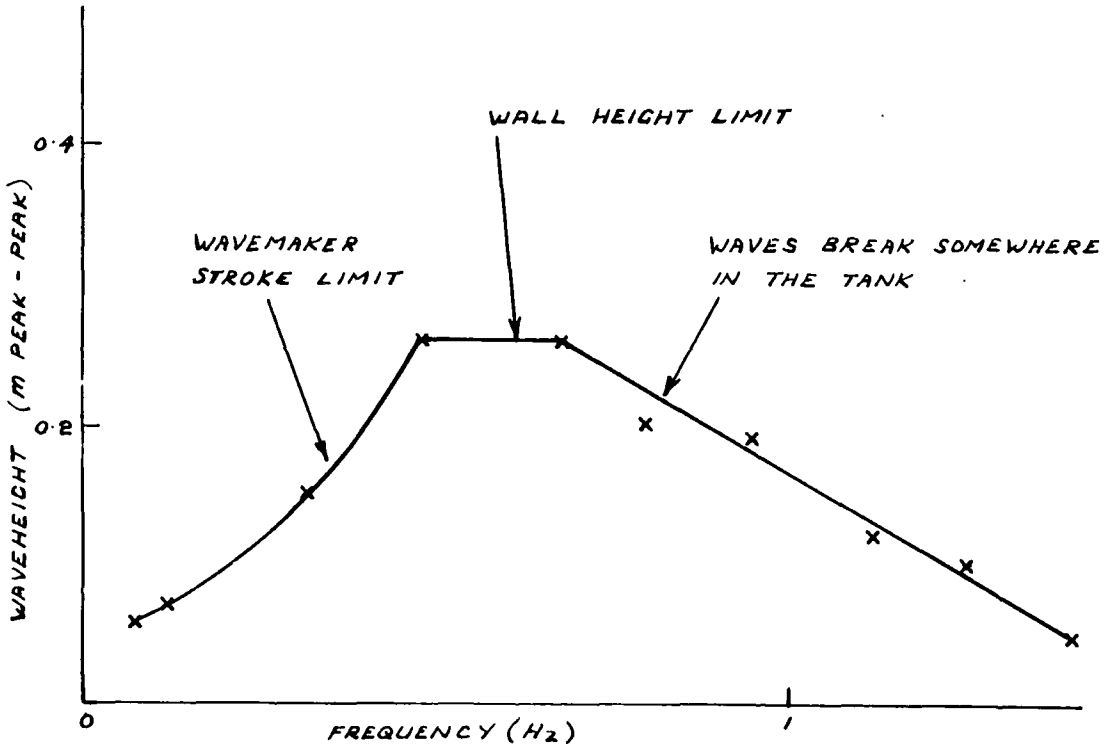

FIG. 4·5. No. 1 SHIP TANK – MEASURED PERFORMANCE LIMITS

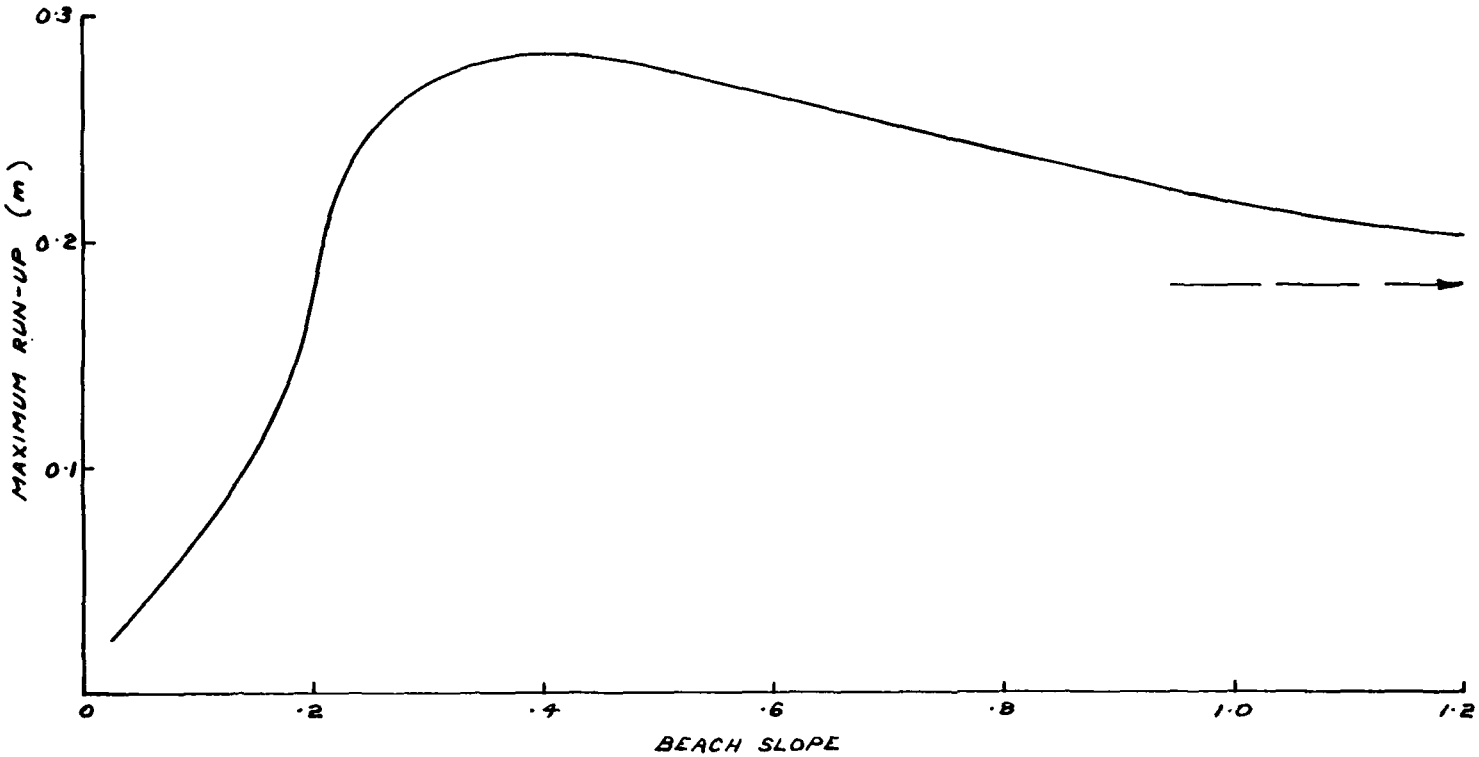

FIG. 5·1. MAXIMUM RUN UP ON PLANE BEACH

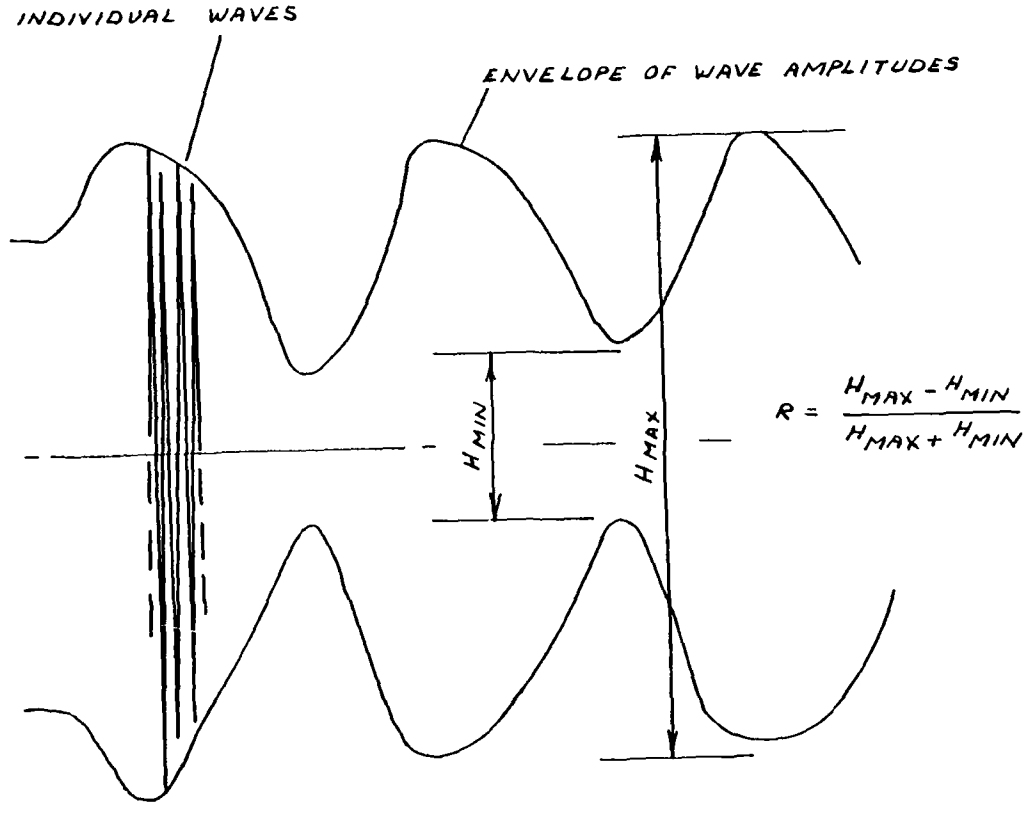

FIG. 5·2. MEASURING BEACH REFLECTION COEFFICIENT – STANDING WAVE METHOD

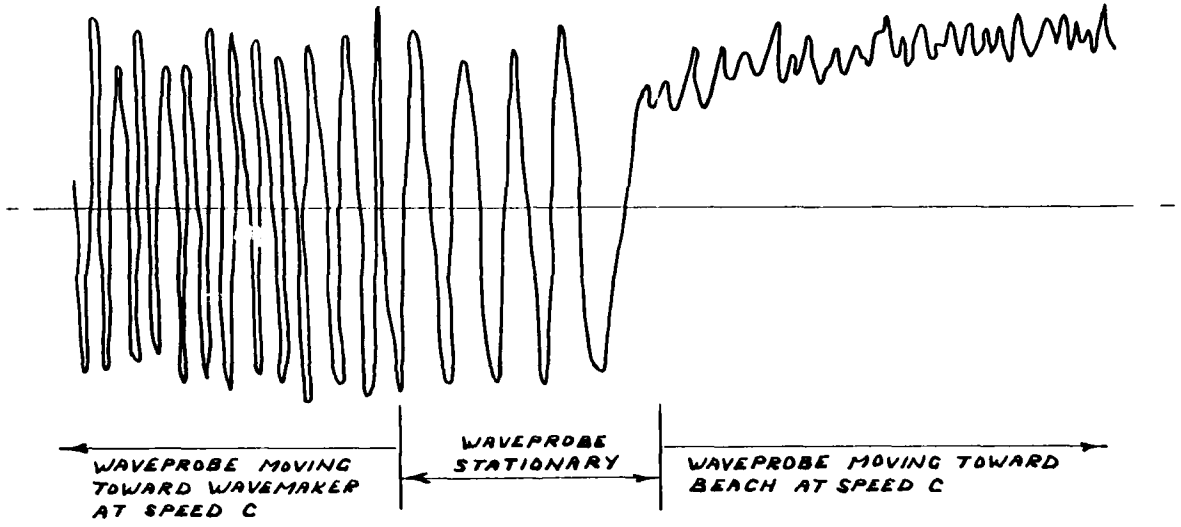

FIG. 5·3. MEASURING BEACH REFLECTION COEFFICIENT – DOPPLER SHIFT METHOD

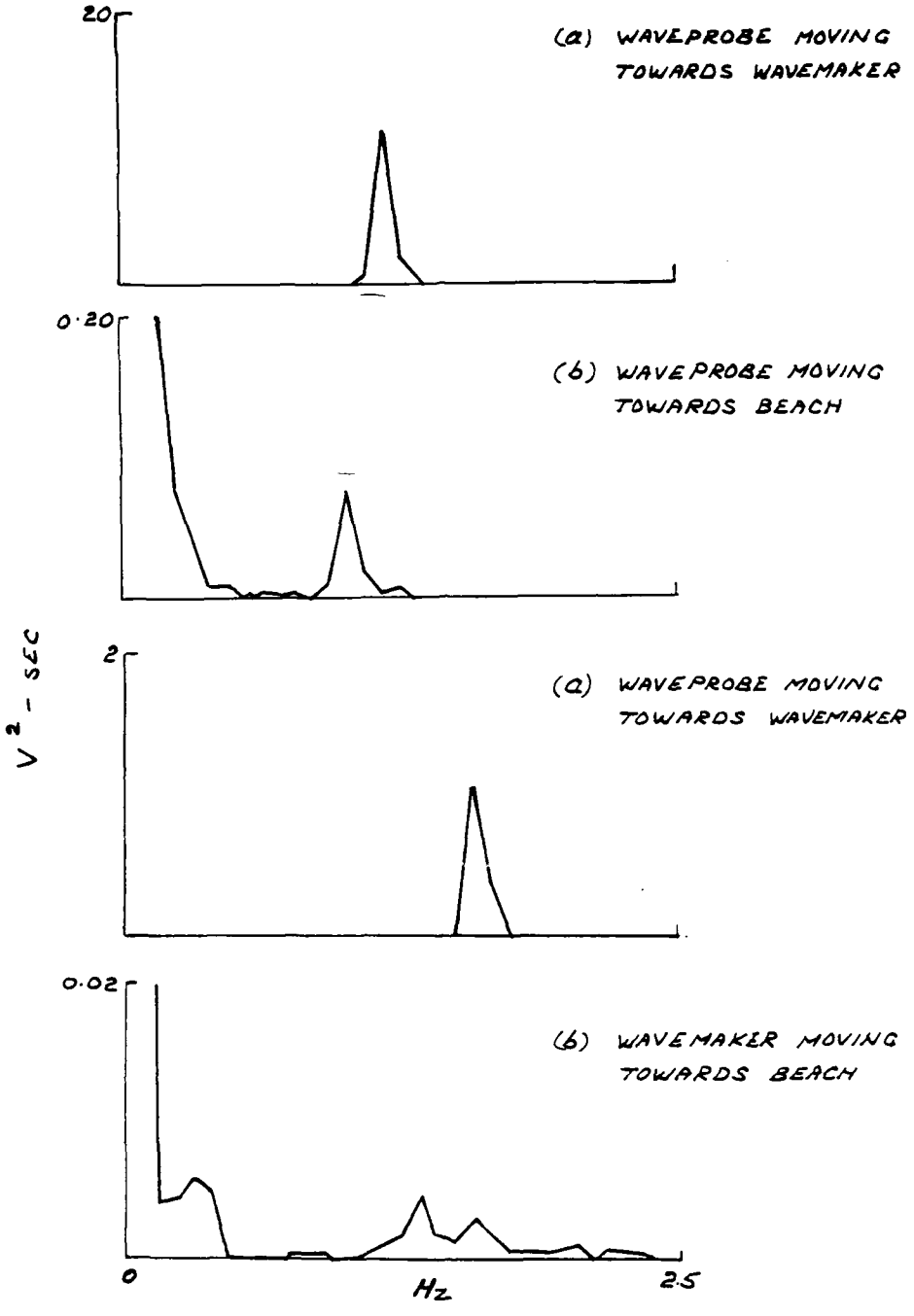

FIG. 5·4. SPECTRA OF OUTPUT FROM MOVING WAVEPROBE

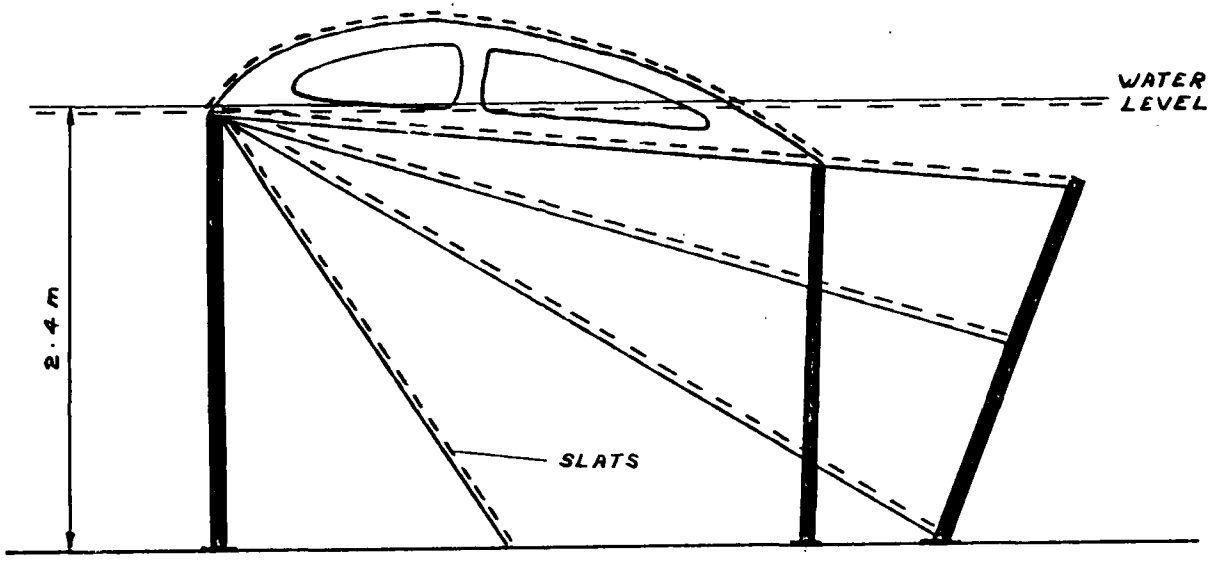

FIG. 5·5. No. 1. SHIP TANK – ORIGINAL BEACH

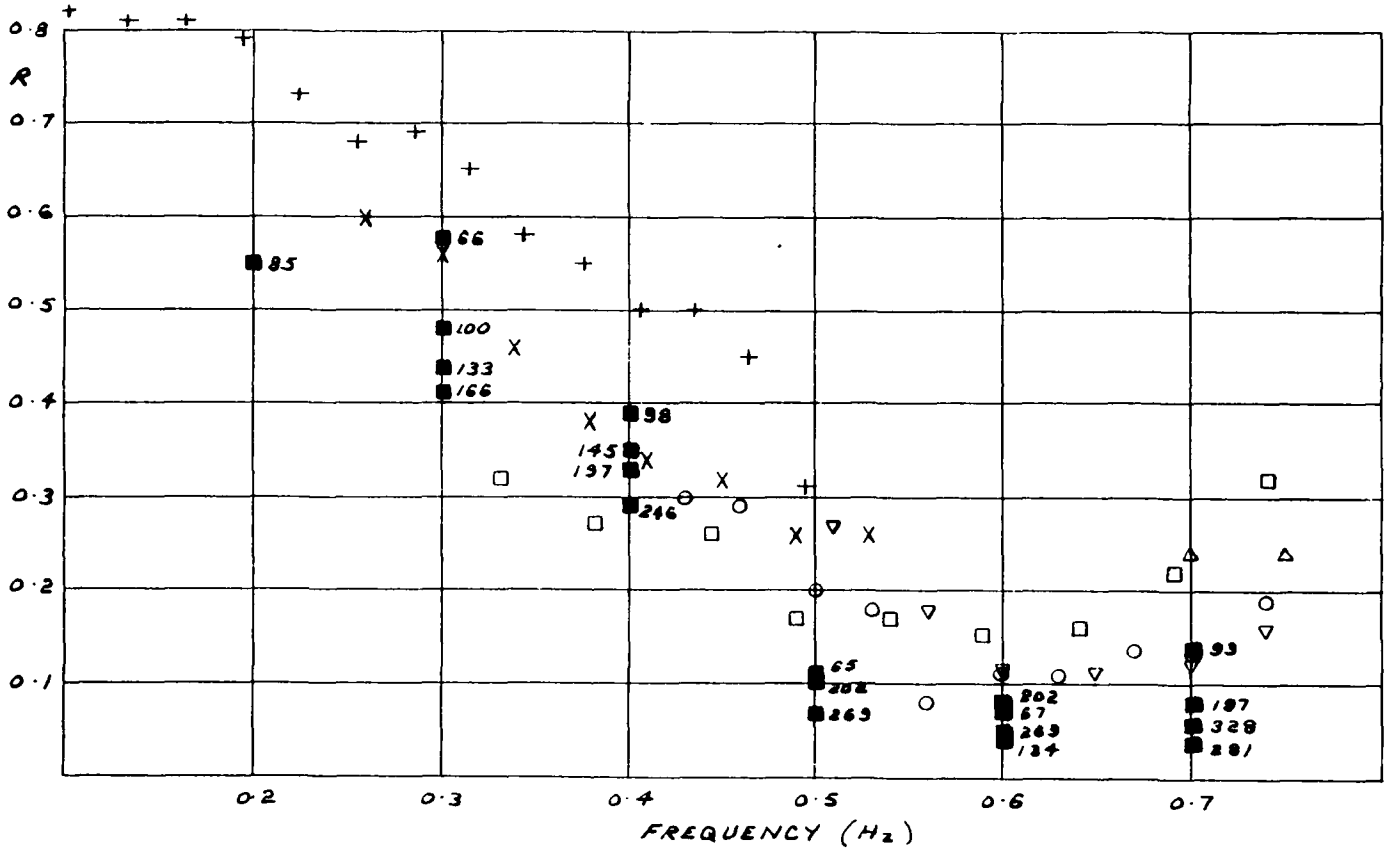

FIG. 5·6. REFLECTION COEFFICIENT OF ORIGINAL BEACH

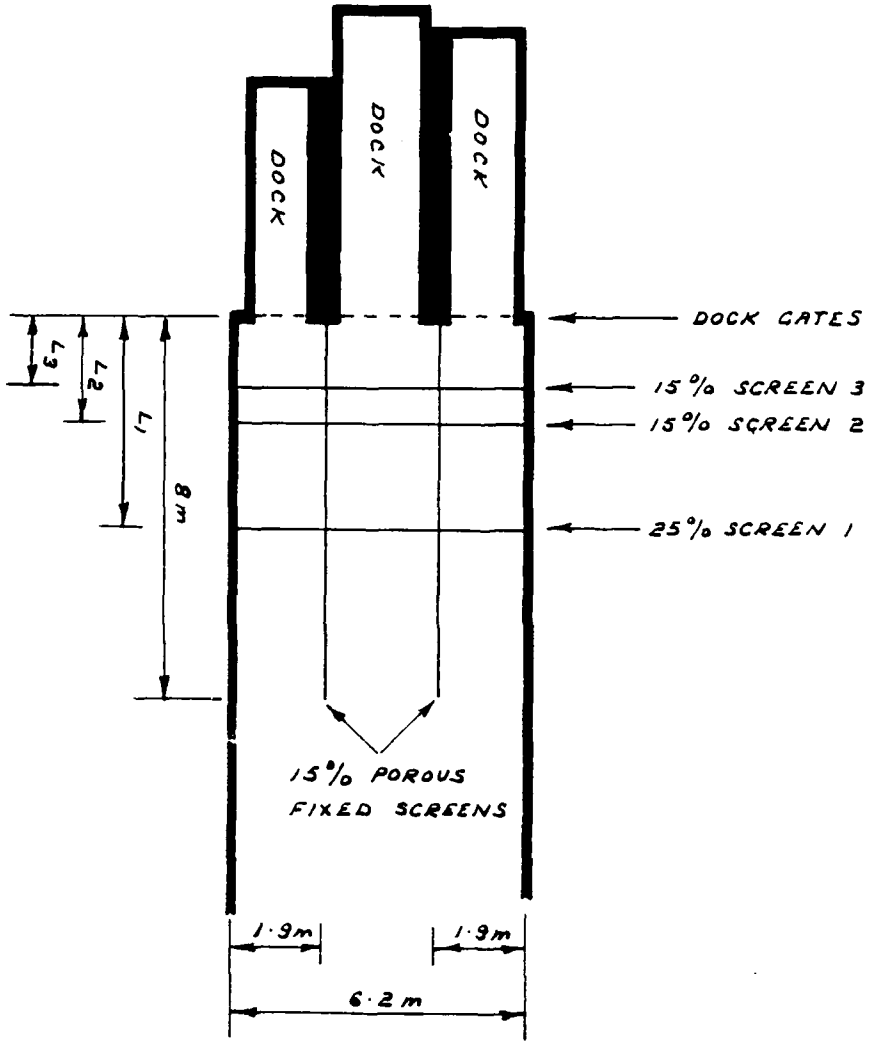

FIG.5·7. PLAN VIEW OF FINAL DESIGN OF ABSORBER

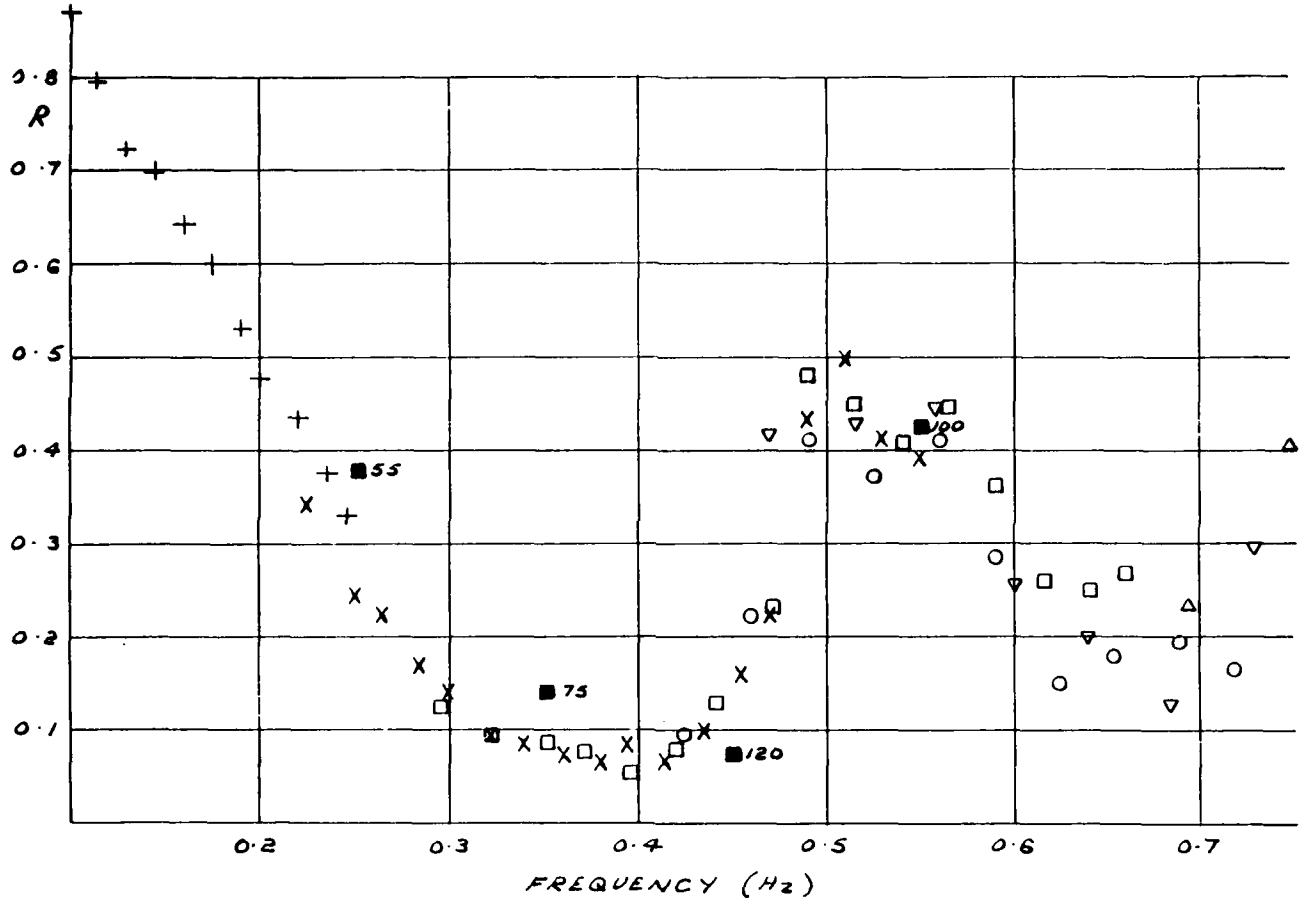

FIG. 5·8 REFLECTION COEFFICIENT OF 3-SCREEN ABSORBER

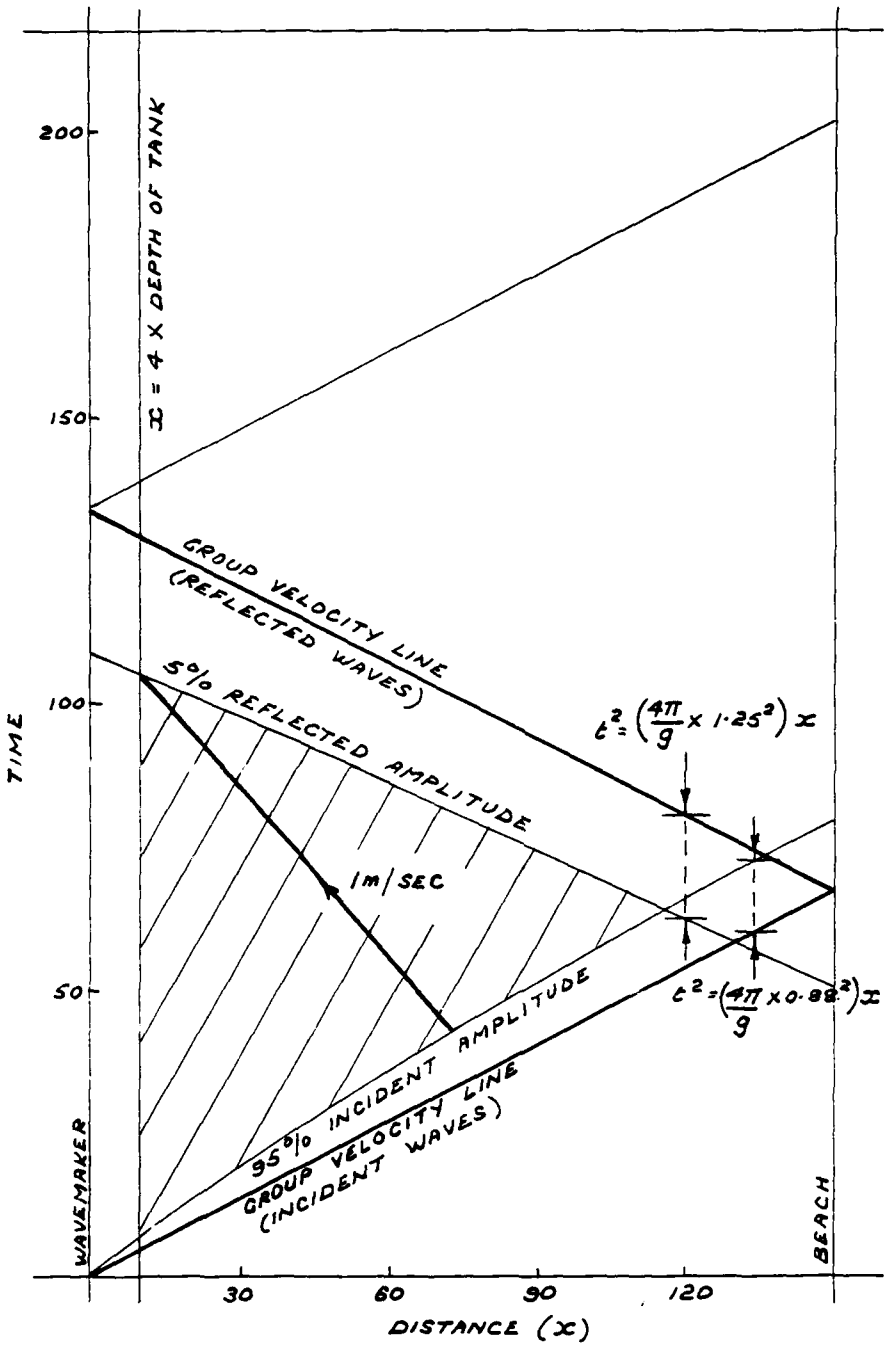

FIG. 6-1. USEFUL LENGTH OF TANK – REGULAR WAVES

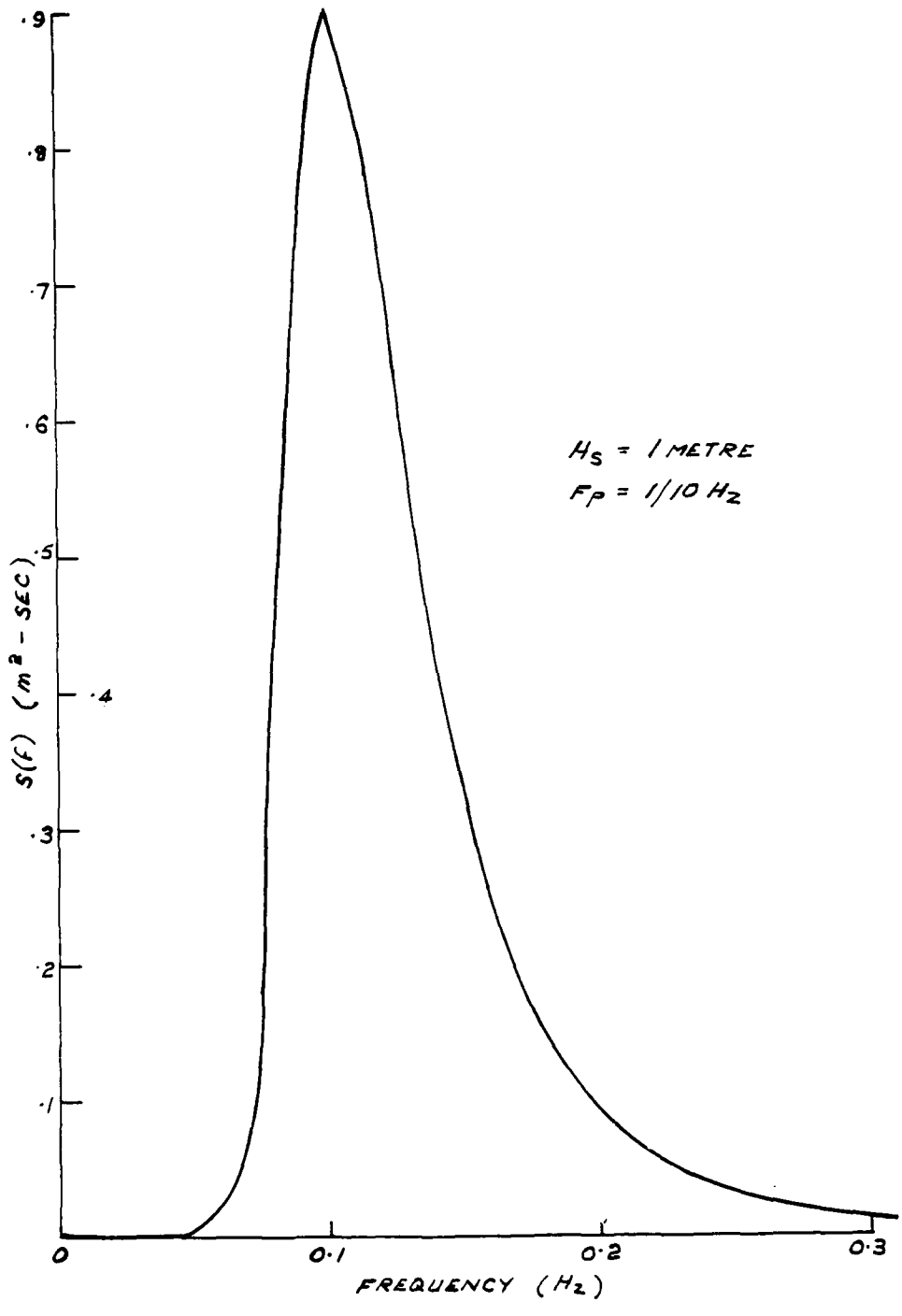

FIG. 7·1 BRETSCHNEIDER SPECTRUM

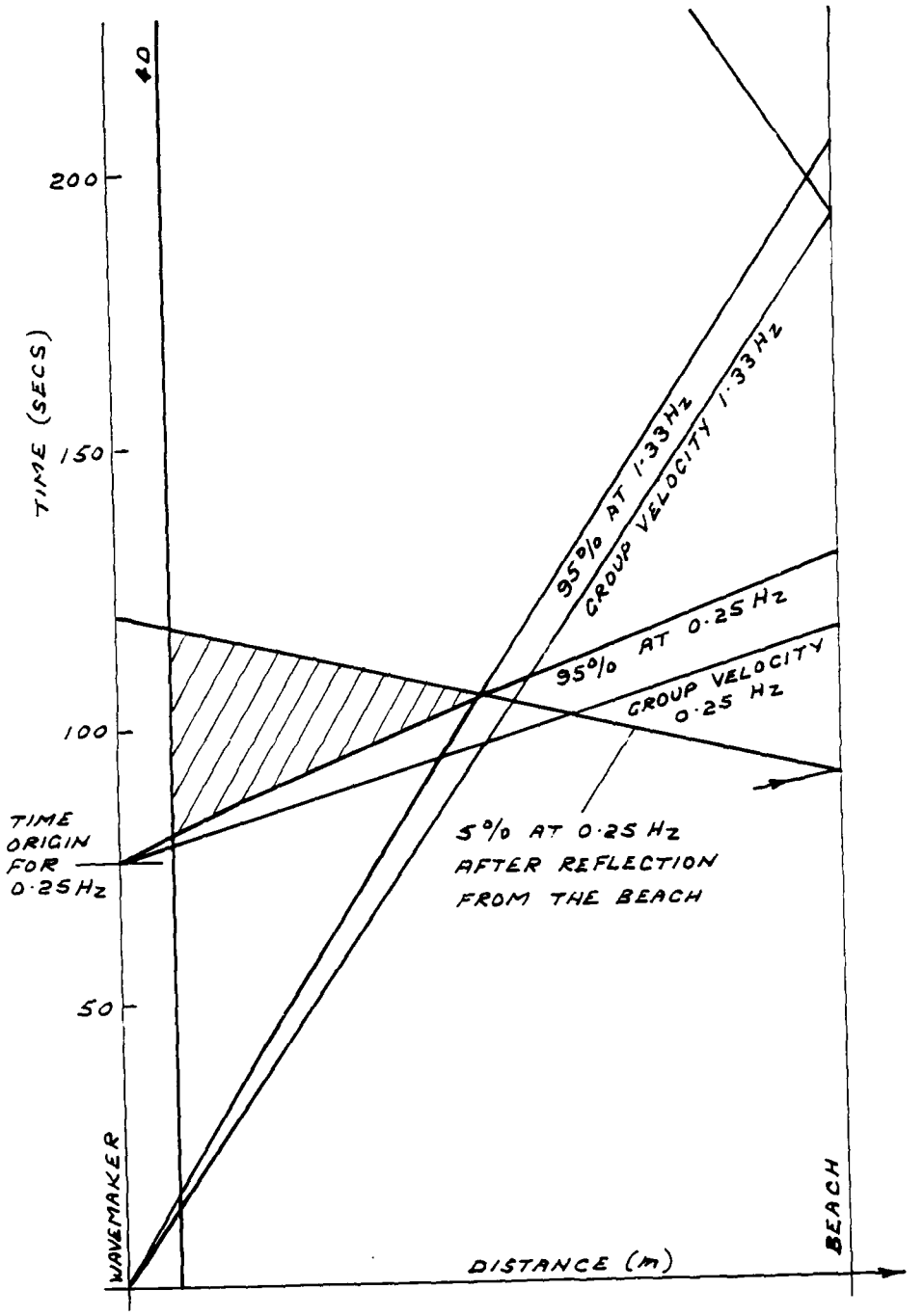

FIG. 9·1. USEFUL LENGTH OF TANK – RANDOM WAVES

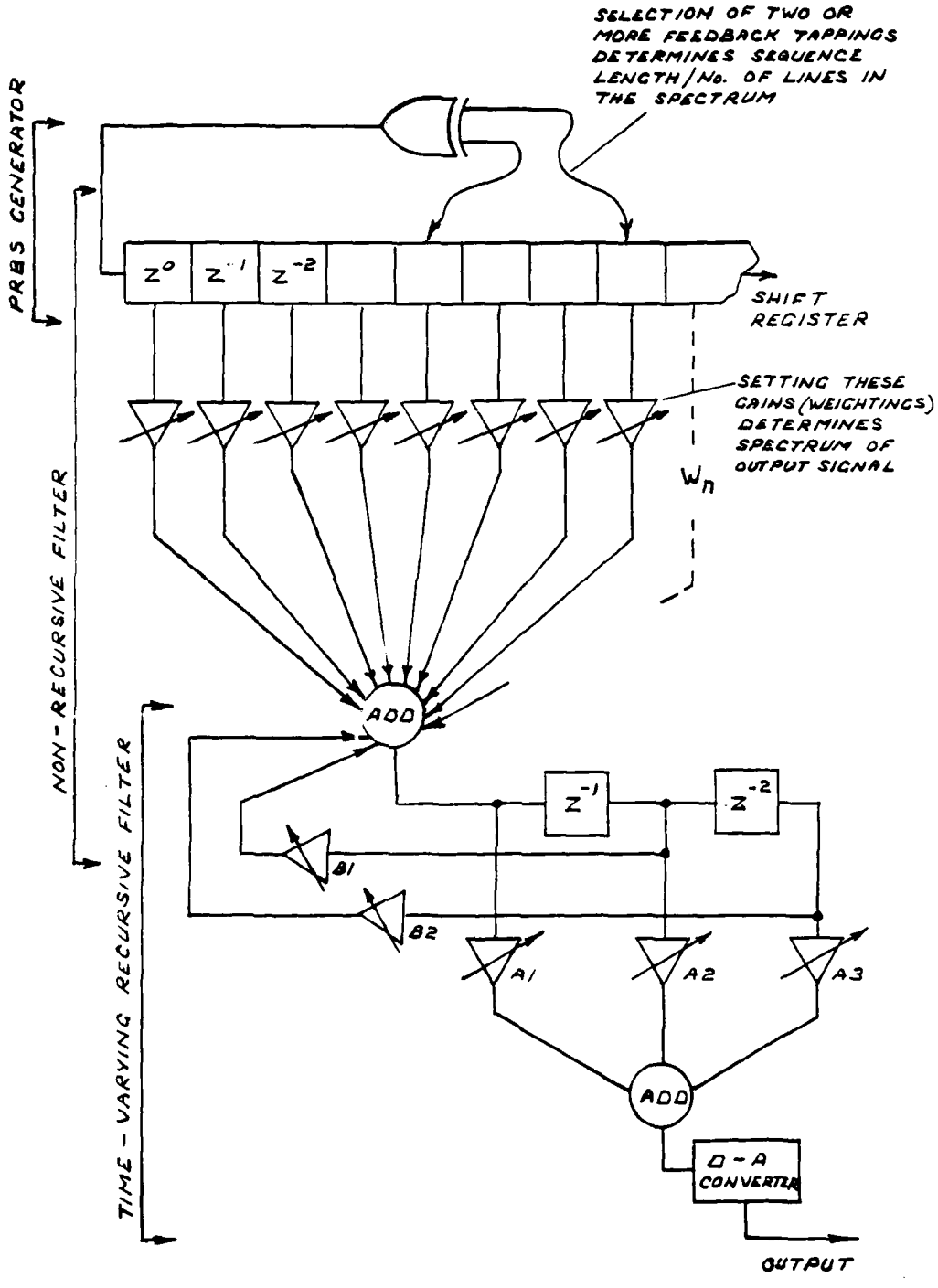

FIG. 10-1. SPECTRUM SYNTHESIZER FOR SHIP TANK

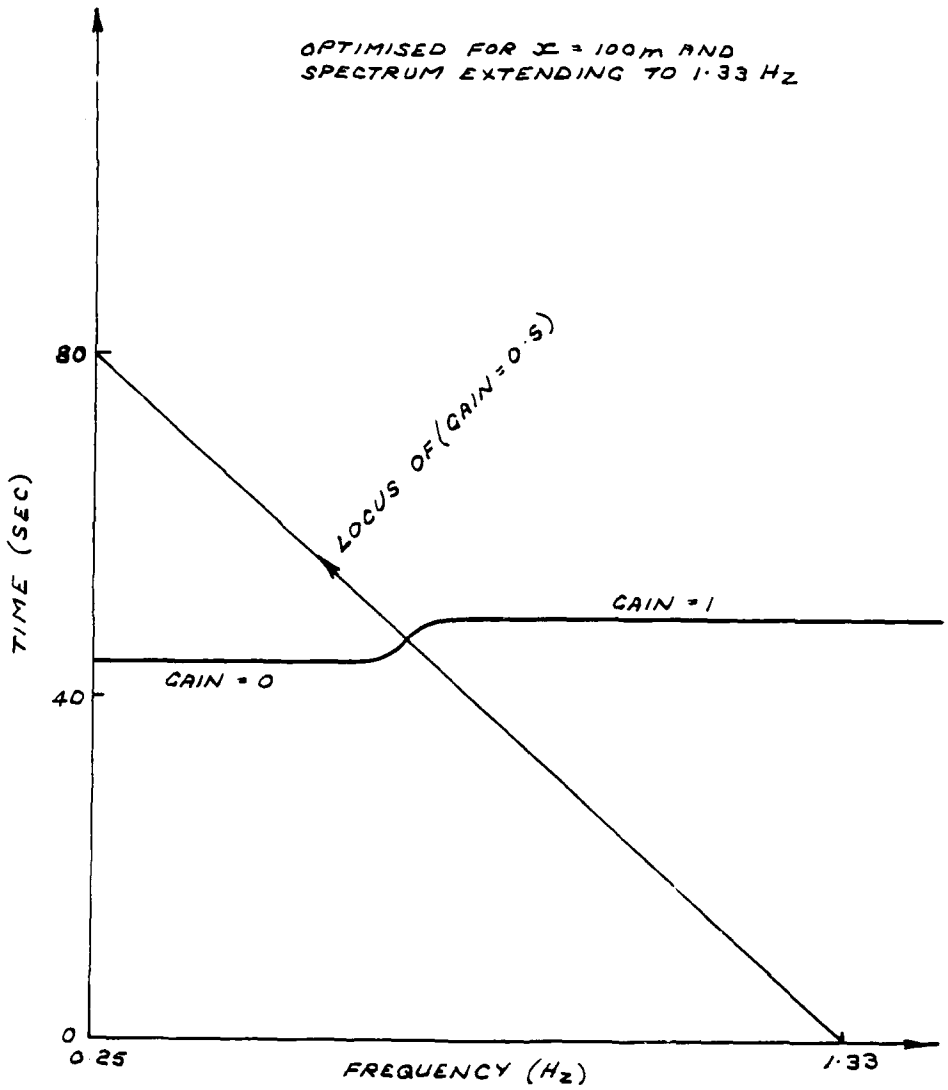

FIG. 10.2. TIME-VARYING FILTER

Appendix 1

MEAN KINETIC ENERGY PER UNIT SURFACE AREA

$$KE = \frac{1}{2}\rho \int_{x=0}^{x=\lambda}\int_{z=-D}^{\zeta=o}\left[\dot{\xi}^2 + \dot{\eta}^2\right] dzdx$$

$$\text{now}\quad \dot{\xi} = \frac{\pi H}{T}\frac{\cosh 2\pi\left[\frac{D+\zeta}{\lambda}\right]}{\sinh\left[\frac{2\pi D}{\lambda}\right]}\cos 2\pi\left[\frac{n}{\lambda} - \frac{t}{T}\right]$$

$$\dot{\eta} = \frac{\pi H}{T}\frac{\sinh 2\pi\left[\frac{D+\zeta}{\lambda}\right]}{\sinh\left[\frac{2\pi D}{\lambda}\right]}\sin 2\pi\left[\frac{n}{\lambda} - \frac{t}{T}\right]$$

Therefore at t=o:

$$\dot{\xi}^2 + \dot{\eta}^2 = \left[\frac{\pi H}{T\sinh\left[\frac{2\pi D}{\lambda}\right]}\right]^2\left[\left[\cosh 2\pi\left[\frac{D+\zeta}{\lambda}\right]\cos\frac{2\pi x}{\lambda}\right]^2 + \left[\sinh 2\pi\left[\frac{D+\zeta}{\lambda}\right]\sin\frac{2\pi x}{\lambda}\right]^2\right]$$

$$= \left[\frac{\pi H}{T\sinh\left[\frac{2\pi D}{\lambda}\right]}\right]^2\left[\cosh^2 2\pi\left[\frac{D+\zeta}{\lambda}\right]\cos^2\frac{2\pi x}{\lambda} + \sinh^2 2\pi\left[\frac{D+\zeta}{\lambda}\right]\sin^2\frac{2\pi x}{\lambda}\right]$$

$$= \left[\frac{\pi H}{T\sinh\left[\frac{2\pi D}{\lambda}\right]}\right]^2\left[\cosh^2 2\pi\left[\frac{D+\zeta}{\lambda}\right] - \cosh^2 2\pi\left[\frac{D+\zeta}{\lambda}\right]\sin^2\frac{2\pi x}{\lambda} + \sin^2\left[\frac{D+\zeta}{\lambda}\right]\sin^2\frac{2\pi x}{\lambda}\right]$$

$$= \left[\frac{\pi H}{T\sinh\left[\frac{2\pi D}{\lambda}\right]}\right]^2\left[\cosh^2 2\pi\left[\frac{D+\zeta}{\lambda}\right] - \sin^2\frac{2\pi x}{\lambda}\right]$$

Now: $\int \cosh^2\zeta\,\partial\zeta = \int \cosh\zeta\,\cosh\zeta\,\partial\zeta\epsilon$

$= \int \cosh\zeta\,\partial(\sinh\zeta)$

$= \int \cosh\zeta\,\sinh\zeta - \int \sin\zeta\,\sinh\zeta\,\partial\zeta$

$= \cosh\zeta\,\sinh\zeta = \int \sinh^2\zeta\,\partial\zeta$

$$= \cosh\zeta \sinh\zeta = \int(\cosh^2 + 1)\partial\zeta$$

$$= \cosh\zeta \sinh z - \zeta - \int\cosh^2\zeta \, \partial\zeta$$

Therefore $2\int\cosh^2\zeta \, \partial\zeta = \cosh\zeta \sinh\zeta - \zeta$

$$\int\cosh^2\zeta = \frac{1}{2}\left[\cosh\zeta \sinh\zeta - \zeta\right]$$

Therefore $\int_{\xi=-D}^{0} \left[\frac{\Pi H}{T\sinh\left[\frac{2\Pi D}{\lambda}\right]}\right]^2 \left[\cosh^2\left[D+\zeta\right] - \sin^2\frac{2\Pi}{\lambda}\left[x\right]\right]\partial\zeta$

$$= \left[\frac{\Pi H}{T\sinh\left[\frac{2\Pi D}{\lambda}\right]}\right]^2 \cdot \left[\frac{1}{2}\frac{\lambda}{2\Pi}\left[\cosh\frac{2\Pi}{\lambda}(D+\zeta)\sinh\frac{2\Pi}{\lambda}(D+\zeta) - \frac{2\Pi}{\lambda}(D+\zeta)\right]\right.$$

$$\left. - \zeta \sin^2\frac{2\Pi}{\lambda}\left[x\right]\right]_{-D}^{0}$$

$$= \left[\frac{\Pi H}{T\sinh\left[\frac{2\Pi D}{\lambda}\right]}\right]^2 \left[\frac{\lambda}{4\Pi}\left[\cosh\frac{2\Pi D}{\lambda}\sinh\frac{2\Pi D}{\lambda} - \frac{2\Pi D}{\lambda}\right] + D\sin^2\frac{2\Pi}{\lambda}\left[x\right]\right]$$

Now: $\int \sin^2\zeta\partial\zeta = \int \sin\zeta\partial\zeta$

$$= -\int \sin\zeta \, \partial(\cos\zeta)$$

$$= -\left[\sin\zeta \cos\zeta - \int \cos\zeta \, \lambda(\sin\zeta)\right]$$

$$= -\left[\sin\zeta \cos\zeta - \int \cos^2\zeta \, \partial\zeta\right]$$

$$= -\left[\sin\zeta \cos\zeta - \int(1 - \sin^2\zeta)\partial\zeta\right]$$

$$= -\left[\sin\zeta \cos\zeta - \zeta + \int \sin^2\zeta\partial\zeta\right]$$

Therefore $2\int\sin^2\zeta\partial\zeta = \zeta = \sin\zeta \cos\zeta$

Therefore $\int\sin^2\zeta\partial\zeta = \frac{1}{2}\left[\zeta - \sin\zeta \cos\zeta\right]$

Therefore

$$\frac{1}{2}\rho \cdot \left[\frac{\Pi H}{T\sinh\left[\frac{2\Pi D}{\lambda}\right]}\right]^2 \int_{x=0}^{\lambda} \left[\frac{\lambda}{4\Pi}\left[\cosh\frac{2\Pi D}{\lambda}\sinh\frac{2\Pi D}{\lambda} - \frac{2\Pi D}{\lambda}\right] + D\sin^2\frac{2\Pi}{\lambda}(x)\right]\partial x$$

$$= \frac{\rho}{2}\left[\frac{\Pi H}{T\sinh\left[\frac{2\Pi D}{\lambda}\right]}\right]^2 \left[\frac{\lambda}{4\Pi}\left[\cosh\frac{2\Pi D}{\lambda}\sinh\frac{2\Pi D}{\lambda} - \frac{2\Pi D}{\lambda}\right]\right.$$

$$\left. + \frac{D\lambda}{4\Pi}\left[\frac{2\Pi x}{\lambda} - \sin\frac{2\Pi x}{\lambda}\cos\frac{2\Pi x}{\lambda}\right]\right]_{x=0}^{\lambda}$$

$$= \frac{\rho}{2}\left[\frac{\Pi H}{T\sinh\left[\frac{2\Pi D}{\lambda}\right]}\right]^2 \left[\frac{\lambda^2}{4\Pi}\left[\cosh\frac{2\Pi D}{\lambda}\sinh\frac{2\Pi D}{\lambda} - \frac{2\Pi D}{\lambda}\right]\right.$$

$$\left. + \frac{D\lambda}{4\Pi}\left[2\Pi - \sin 2\Pi\cos 2\Pi\right]\right]$$

$$= \frac{\rho}{2}\left[\frac{\Pi H}{T\sinh\left[\frac{2\Pi D}{\lambda}\right]}\right]^2 \left[\frac{\lambda^2}{4\Pi}\left[\cosh\frac{2\Pi D}{\lambda}\sinh\frac{2\Pi D}{\lambda}\right] - \frac{D\lambda}{2} + \frac{D\lambda}{2}\right]$$

$$= \frac{\rho}{2}\left[\frac{\Pi H}{T\sinh\left[\frac{2\Pi D}{\lambda}\right]}\right]^2 \left[\frac{\lambda^2}{4\Pi}\left[\cosh\frac{2\Pi D}{\lambda}\sinh\frac{2\Pi D}{\lambda}\right]\right]$$

$$= \frac{\rho}{2}\left[\frac{\Pi H}{T}\right]^2 \left[\frac{\lambda^2}{4\Pi} \cdot \frac{\cosh\frac{2\Pi D}{\lambda}}{\sinh\frac{2\Pi D}{\lambda}}\right]$$

$$= \frac{\rho\Pi^2 H^2 \lambda^2}{8\,\Pi\,T^2\tanh\frac{2\Pi D}{\lambda}}$$

$$\left[\text{But } \frac{\lambda^2}{T^2} = C^2 = \frac{g\lambda}{2\Pi}\tanh\frac{2\Pi D}{\lambda}\right]$$

Therefore $KE = \frac{\rho g H^2 \lambda}{16}$

Appendix 2

PROPAGATION OF THE INITIAL WAVES

When the wavemaker running at monofrequency (fo) is started up extra frequencies are introduced on either side of the main carrier frequency. As the front travels down the tank these frequencies will disperse so that, for instance, a sudden step start will produce a much slower build up to the final constant amplitude at some distance (x) down the tank. This effect will be calculated for a general start up condition. In doing this it is much easier to assume that all the waves obey the deep water dispersion equation.

The calculation uses the fourier transform pair:

$$x(t) = \int_{-\infty}^{\infty} a(f)e^{-2\pi ift}df$$

$$a(f) = \int_{-\infty}^{\infty} u(t)e^{2\pi ift}dt$$

If this pair is written $u(t) \leftrightarrow a(f)$

and if $y(t) \leftrightarrow b(f)$

then these properties hold and $u(t-t_o) \leftrightarrow e^{2\pi ift_o}\, a(f)$

will be used in what follows $u(t)e^{-2\pi if_o t} \leftrightarrow a(f-f_o)$

$$\dot{u}(t) \leftrightarrow -2\pi ifa(f)$$

$$u(t)*y(t) \leftrightarrow a(f)b(f)$$

(where * denotes the convolution $\int_{-\infty}^{\infty} u(\tau)y(t-\tau)d\tau$).

Let g(t) be a function centred about t = 0 of area unity (Figure A1).

Integrate to give the wave envelope at the paddle (Figure A2).

Take a monofrequency wave (fo) with this envelope as illustrated in Figure A3.

At distance (x) down the tank $e^{-2\pi ift} \rightarrow e^{2\pi i(kx-ft)}$
where k is given by the dispersion equation k = k(f).

Hence if $U_x(t)$ is the wave form at this position:

$$u_x(t) \leftrightarrow -\frac{G(f-f_o)}{2\pi i(f-f_o)}\, e^{2\pi ikx}$$

Assuming deep water conditions $f^2 = \frac{gk}{2\pi}$ and the group velocity is

$V(f) = \frac{df}{dk} = \frac{g}{4\pi f}$. Hence

$$k = \frac{2\pi f^2}{g} = k_o + \frac{(f-f_o)}{V(f_o)} + \frac{2\pi}{g}(f-f_o)^2$$

where $k_o = \frac{2\pi f_o^2}{g}$. Therefore

$$U_x(t) = y(t-t_o)e^{2\pi i(kx-f_o t)} \text{ where}$$

$$y(t) \leftrightarrow -\frac{G(f)}{2\pi i f} e^{2\pi i \frac{2\pi x f^2}{g}}$$

So that y(t) gives the shape of the envelope of the monofrequency wave at x and $t_o = \frac{x}{v(f_o)}$ is the time delay on the envelope due to the group velocity of the carrier wave.

Notice that the envelope shape is independent of the carrier frequency.

Now consider first of all, the case where the generator is instantaneously switched on. Then $g_1(t) = \delta(t)$ (Dirac delta function). Hence $G_1(f) = 1$.

$$\text{With } y(t) \leftrightarrow -\frac{G(f)}{2\pi i f} e^{2\pi i \frac{2\pi d f^2}{g}}$$

$$\text{then } y(t) = \int_{-\infty}^{t} z(t)dt$$

$$\text{where } z(t) \leftrightarrow G(f)\, e^{\pi i b^2 f^2} \qquad b^2 = \frac{4\pi x}{g}$$

$$\text{If } G_1(f) = 1 \text{ then } z_1(t) = \int_{-\infty}^{\infty} e^{\pi i(b^2 f^2 - 2ft)} df$$

$$= e^{-\pi i t^2/b^2} \int_{-\infty}^{\infty} e^{\pi i(bf - t/b)^2} df$$

$$\text{put } bf - t/b = \phi$$

$$= \frac{1}{b} e^{-\pi i t^2/b^2} \int_{-\infty}^{\infty} e^{i\pi\phi^2} d\phi$$

$$= \frac{1}{b} e^{\pi i(-t^2/b^2 + \frac{1}{4})}$$

Therefore $y_1(t) = \frac{e^{i\pi/4}}{b} \int_{-\infty}^{t} e^{-\pi i t^2/b^2} dt$ put $t = \frac{b}{\sqrt{2}} \psi$

$$= \frac{e^{i\pi/4}}{\sqrt{2}} \int_{-\infty}^{\tau} e^{-2\pi/2\psi^2} d\psi \quad \tau = \frac{\sqrt{2}t}{b} = \frac{t}{\sqrt{\frac{2\pi x}{g}}}$$

$$= \tfrac{1}{2} + \frac{1+i}{2} \left[C(\tau) - iS(\tau)\right] \qquad (1)$$

If $G_2(f) = e^{-2\pi^2\sigma^2 f^2}$

then $z_2(t) = \int_{-\infty}^{\infty} e^{-2\pi^2\sigma^2 f^2 + \pi i b^2 f^2 - 2\pi i f t} df$

$$= e^{-\pi i t^2/\alpha^2} \int_{-\infty}^{\infty} e^{\pi i(\alpha f - t/\alpha)} df$$

where $\alpha^2 = b^2 + 2\pi i \sigma^2$

$$= \frac{1}{\alpha} e^{\pi i(-t^2/\alpha^2 + \frac{1}{4})} \text{ as above}$$

Therefore $y_2(t) = \frac{1}{\alpha} e^{i\pi/4} \int_{-\infty}^{t} e^{-\pi i t^2/\alpha^2} dt$ put $m^2 = \pi i t^2/\alpha^2$

$$= \frac{1}{\sqrt{\pi}} \int_{-\infty}^{w} e^{-m^2} dm \quad w = \frac{\pi^{\frac{1}{2}} e^{i\pi/4} t}{\alpha} = \frac{t}{\sqrt{\left[2\sigma^2 - i\frac{4x}{g}\right]}}$$

$$= \tfrac{1}{2} (\text{erf} w + 1) \qquad (2)$$

from (1): $y_1(t) = \tfrac{1}{2} + \frac{1+i}{2} \left[C(\tau) - i\, S(\tau)\right]$

Where C-iS is a Fresnel integral of $\tau = \frac{t}{(2\pi x/g)^{\frac{1}{2}}}$.

The complex value of y_1 as a function of τ is a Cornu spiral.

The magnitude of y_1, which gives the shape of the wave envelope, is shown in Figure 9.

Now turning to the generator growing smoothly to its final amplitude take as a representative case a rise along an error function curve, for the actual shape is not important and this one is analytically solvable. Thus the original delta function of g(t) is allowed to widen out into a gaussian curve:

$$g_2(t) = \frac{1}{\sqrt{2\pi}\sigma} e^{-t^2/2\sigma^2}$$

$$\text{Then } G_2(f) = \frac{1}{\sqrt{2\pi}\sigma} \int_{-\infty}^{\infty} e\left[-\frac{t^2}{2\sigma^2} + 2\pi i f t\right] dt$$

$$= e^{-2\pi^2\sigma^2 f^2} \frac{1}{\sqrt{2\pi}\sigma} \int_{-\infty}^{\infty} e^{-\frac{1}{2\sigma^2}(t-2\pi i\,\sigma^2 f)^2} dt$$

$$= e^{-2\pi^2\sigma^2 f^2}$$

from (2): $y_2(t) = \frac{1}{2}(\text{erf}w - 1)$

$$\text{where } w = \frac{t}{\sqrt{2\sigma^2 - i\frac{4x}{g}}}$$

Thus $y_2(t)$ is an error function of a complex variable (w) and as the time changes, w runs along a line of constant phase in the complex plane. When x = 0, w is real and the error function at the generator is recovered and when $\sigma = 0$, w has phase $\pi/4$ and the error function reduces to the Fresnel integrals above. To take an intermediate case choose σ so that

$$\sigma = \sqrt{\frac{2x}{g}}$$

Then w has phase $\pi/8$ half way between these two cases.

$$w = \frac{t}{2^{1.25}(x/g)^{1/2}} e^{i\pi/8}$$

The corresponding smooth rise at the wave generator and the wave envelope given by the magnitude of y_2 is shown as Figure 10. As was to be expected with a smooth input the ripples in amplitude after the central rise are much reduced but what is surprising is that the central rise itself is not spread over a greater time, but is acutally very much sharper. This is because the smoothing is effectively done on the complex Cornu spiral before extracting the amplitude and here the various phases can cancel out upon smoothing.

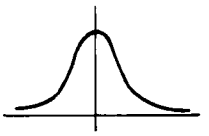

FIG. A1

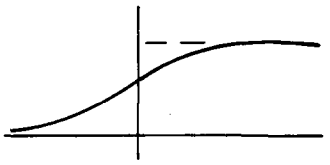

FIG. A2

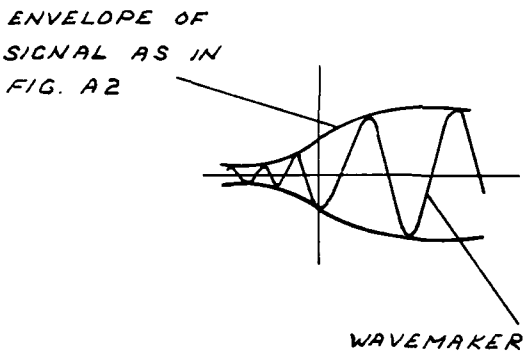

FIG. A3

Distribution

Copy Numbers	
	D Sc(SEA) (Abstract Only)
1-3	Deputy Controller (Warships) CNA/NA 122
4	Director ARE
5	Deputy Director Submarine and Underwater Systems, ARE
6	Head of Hydrodynamics and Structures Department, ARE
7	Staff Officer (C) BNS
8-13	US Navy Technical Liaison Officer
14	SM211 (Mr K Monk)
15	Marine Sciences Group 5 Hydrographic Dept (Mr N Gooding)
16	CS(R)2e (Navy)
17-41	DRIC
43-44	Library ARE Portsdown
45-46	Library ARE Portland

Document Control Sheet

Overall security classification of sheet **UNCLASSIFIED**

(As far as possible this sheet should contain only unclassified information. If it is necessary to enter classified information, the box concerned must be marked to indicate the classification eg (R), (C) or (S)).

1. DRIC Reference (if known)	2. Originator's Reference ARE TR89311
3. Agency Reference	4. Report Security Classification UNLIMITED
5. Originator's Code (if known)	6. Originator (Corporate Author) Name and Location **ADMIRALTY RESEARCH ESTABLISHMENT** **HASLAR, GOSPORT, HANTS, PO12 2AG**
5a. Sponsoring Agency's Code (if known)	6a. Sponsoring Agency (Contact Authority) Name and Location

7. Title
WAVES IN SHIP TANKS
PART 1: GENERATING A RANDOM SEA

7a. Title in Foreign Language (in the case of translations)

7b. Presented at (for conference papers). Title, place and date of conference

8. Author 1. Surname, Initials	9a. Author 2	9b. Authors 3,4..	10. Date pp ref
FRYER D K			7.1989 13

11. Contract Number	12. Period	13. Project	14. Other References

15. Distribution Statement
UNLIMITED

Descriptors (or keywords)
MODELLING
SEA
SEA STATE

Abstract
This report describes the difficulties encountered when modelling regular and random seas in ship tank. A method of experiment design which minimises the errors in the sea state is proposed. One implementation of the method is described in some detail.